- CHAPTER 2 -

SYNCHRONOUS MACHINE BEHAVIOUR DURING OUT-OF-STEP OPERATION

*"The fine line between living in a dreamworld, and living your **D**ream, separates the dreamers from the high fliers."*
Lafras Lamont

2.1 INTRODUCTION

This chapter discusses the basic theory of synchronous machines. Machine conventions are reviewed to determine the signs of variables like torque, speed and others to be used in the pole-slip protection function. The effect of saliency is investigated as well as detailed derivations of the machine power angle.

Basic machine parameters are determined from simulated data in order to clarify how these parameters will be used in the pole-slip protection function. The operation of synchronous machines is explained to clarify how machine stability is maintained.

A basic approach to excitation systems is also given to understand the transient response of the machine EMF during disturbances. The calculation of the machine transient EMF is presented, since this forms part of the new pole-slip protection function.

Shaft torque during pole-slip scenarios is investigated to determine the mechanical stress effect of pole slipping on machine shafts. Sub-synchronous resonance is also briefly reviewed.

2.2 SYNCHRONOUS MACHINE CONVENTIONS

It is important to choose a generally accepted synchronous machine convention to determine what the sign of the active and reactive power as well as the power angle must be for synchronous motors and generators. The IEC 60034-10 standard gives the following guidelines on synchronous machine conventions [3]:

a) When the generator convention is taken as a base, active power (P) is considered as positive when it flows from the generator to the network (load). In cases when the motor convention is taken as a base, the active power drawn from a source of electric energy is considered as positive.

b) A synchronous machine is operated with positive reactive power when overexcited for generator convention (lagging power factor), and when underexcited for motor convention (leading power factor). In other words, the positive value of reactive power (Q) corresponds to the reference direction of active power (P).

c) All torques accelerating the rotating parts in the positive direction of rotation are taken as positive. For a generator, the prime mover torque is positive and the generator electromagnetic torque is negative. For motor operation, the shaft (load) mechanical torque is taken as negative and the motor electromagnetic torque is taken as positive.

d) Slip is considered as positive when the speed of rotor rotation is below synchronous speed (motor operation). Slip is considered as negative when rotor rotation is above synchronous speed (generator operation).

e) Excitation voltage is positive when it produces positive field current

The developed pole-slip protection function will use the *generator convention* as a base.

Some clarification on the power factor (Φ) and active and reactive power for both generator and motor conventions are given in Figure 2.1. The arrow shown with the power factor angle Φ as indicated in Figure 2.1 should always point from I to V along the shortest way. If this direction is clockwise, then Φ is negative.

Power angle measurements for both generator and motor conventions as a base are shown in Figure 2.2. The arrow shown with the power angle δ should point along the shortest way from phasor V to the positive quadrature-axis direction in the case of generator convention as a base, and from the negative quadrature-axis direction to phasor V when the motor convention is used as a base.

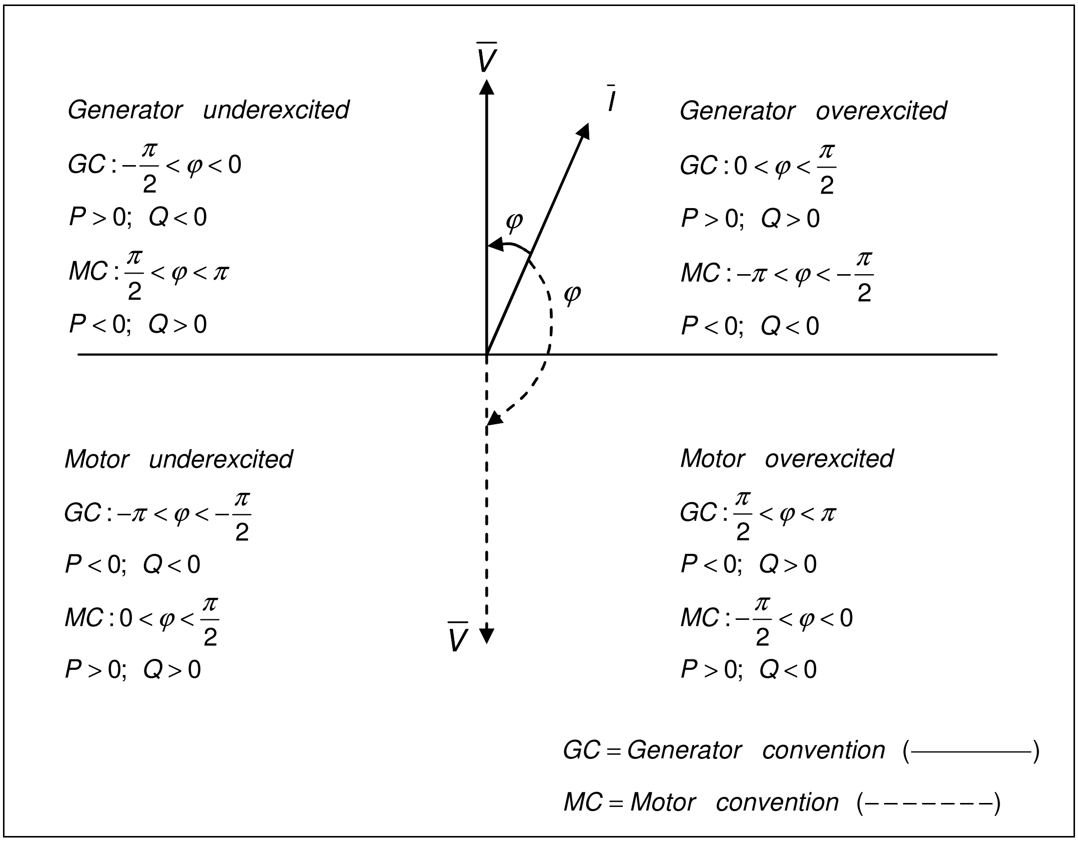

Figure 2.1: Voltage and current phasors in generator and motor convention systems [2]

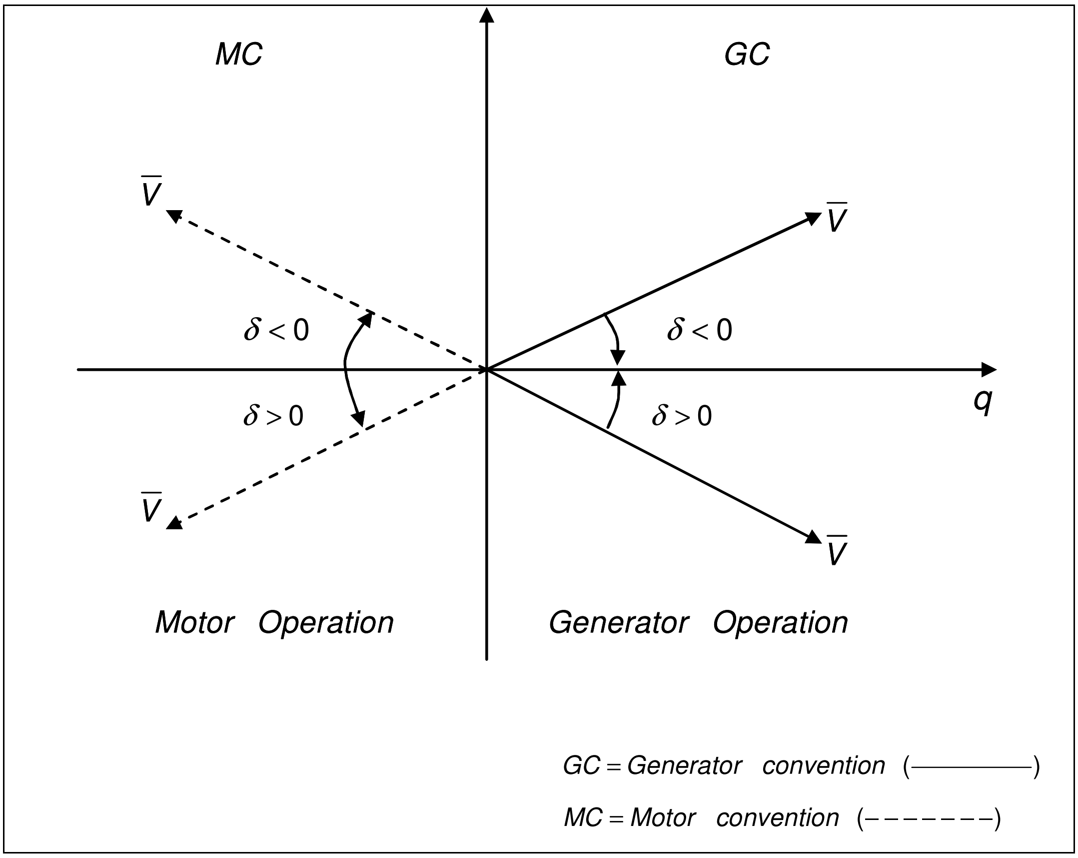

Figure 2.2: Reference diagram for power angle δ measurements [2]

2.3 Capability Diagrams

The capability diagram of a synchronous machine illustrates the electrical limits where the machine can operate. With the terminal voltage V_a and synchronous reactance X_s known, there are six operating variables namely *P, Q, δ, Φ,* I_a and E_f. The selection of any two quantities such as *Φ* and I_a, *P* and *Q* or *δ* and E_f determines the operating point of the other four quantities [4].

It can be shown that the real- and reactive powers of a synchronous machine can be plotted in the complex S-plane with the locus of a circle with radius $\frac{|V_a||E_f|}{|X_s|}$ [4]. The centre of the locus will be at (0, - $\frac{|V_a|^2}{|X_s|}$) as shown in Figure 2.3.

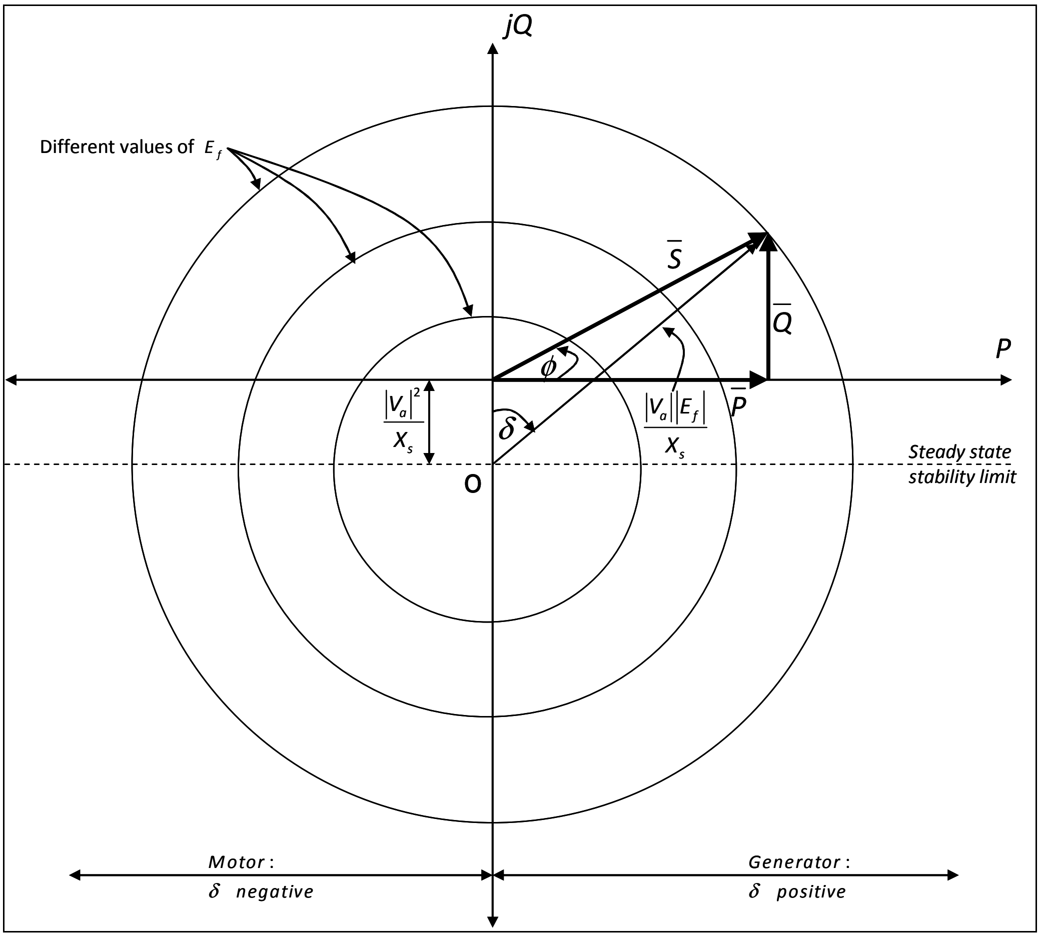

Figure 2.3: Complex power locus [4]

The power angle *δ* and power factor *Φ* are indicated for a chosen operating point. The different circles shown in Figure 2.3 correspond to various excitation voltages E_f. The locus of the maximum power representing the steady-state limit is a horizontal line for which $\delta = 90^{o}$.

A synchronous machine cannot be operated at all points inside the circle for a given excitation E_f (Figure 2.3) without exceeding the machine rating. The region of operation is restricted by the following limitations [4]:

- Armature heating due to the armature current
- Field heating due to the field current
- Steady-state stability limit
- Overheating of the end stator core

The capability curves that define the limiting region for each of the above considerations can be drawn for a constant terminal voltage V_a. The circle in Figure 2.4 with centre at the origin 0 and radius $S = V_a \cdot I_a$ defines the region of operation for which armature heating will not exceed a specific limit.

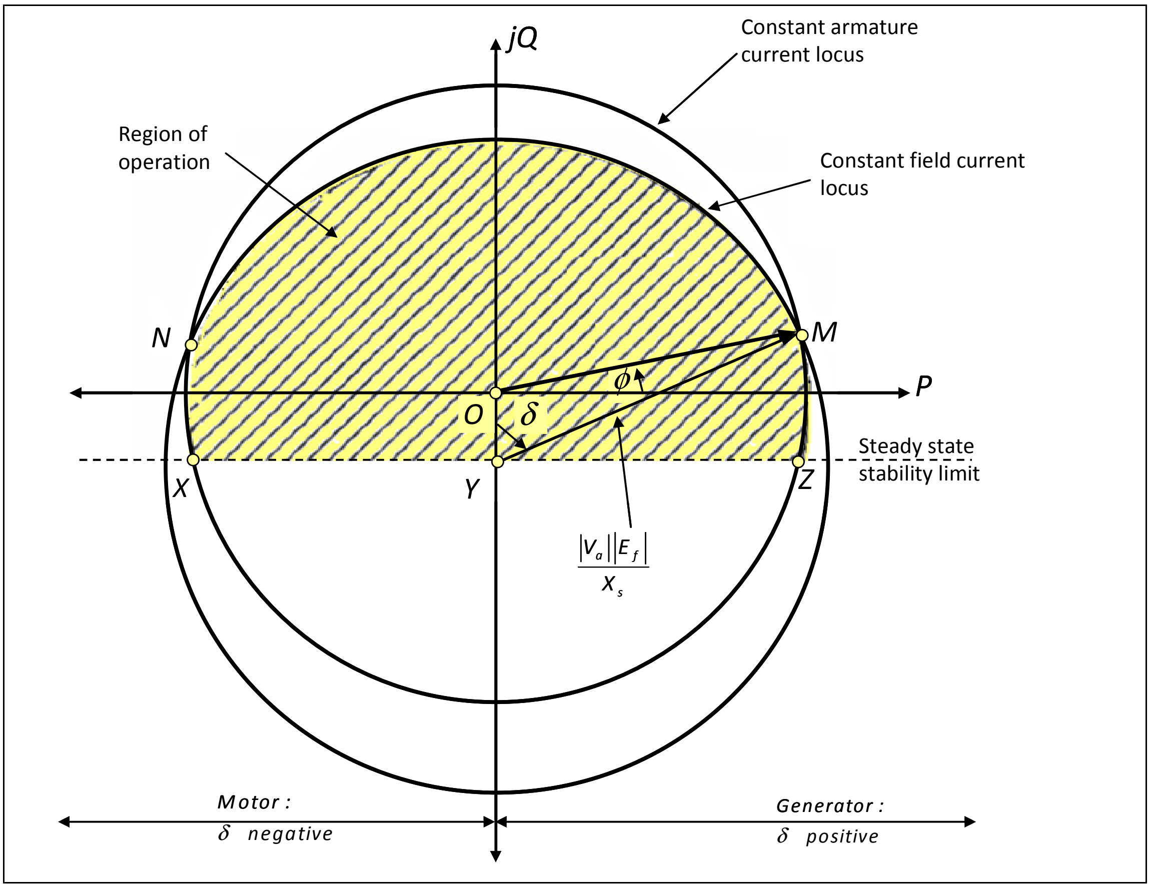

Figure 2.4: Capability curves of a synchronous machine [4]

The circle with centre at (0, - $\frac{|V_a|^2}{|X_s|}$) and radius $\frac{|V_a||E_f|}{|X_s|}$ defines the region of operation for which field heating will not exceed a specific limit. The horizontal line XYZ represents the steady-state stability limit for which $\delta = 90^o$.

The shaded area bounded by the three capability curves defines the area of operation of a synchronous machine. The intersecting points M (for generator) and N (for motor) of the armature heating- and field heating curves determine the optimum operating points. Operation at points M and N maximises the utilization of the armature and field circuits [4].

Figure 2.5 shows the capability diagram of a 38 MVA synchronous generator with P on the y-axis and Q on the x-axis. A leading power factor in the generator convention implies an underexcited machine. For underexcited conditions, the practical stability limit determines the operating range. For overexcited conditions (lagging power factor), the rotor field current heating limit determines the operating range.

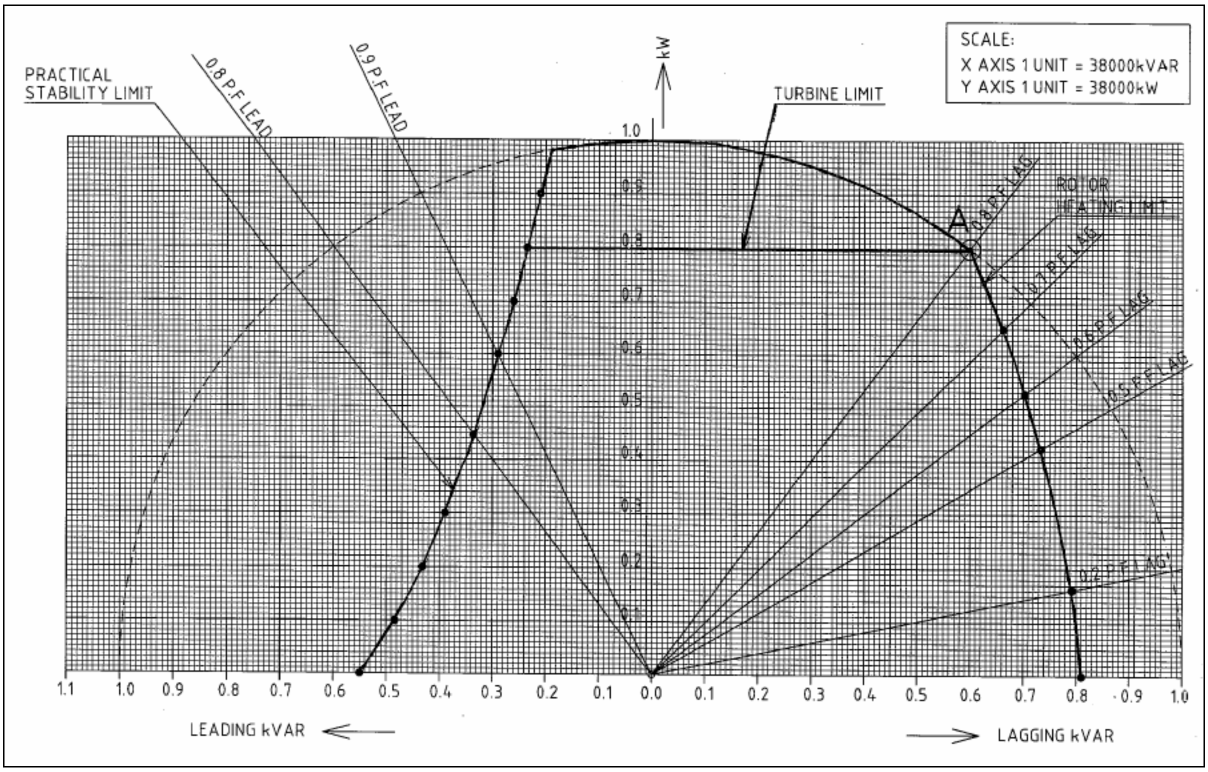

Figure 2.5: Capability curves of a 38 MVA synchronous generator (Courtesy: TD Power Systems)

On the y-axis, the turbine mechanical power limit determines the operating limit. In this example the prime mover mechanical power limit is 0.8 pu. The active power P is normally less than the MVA rating and is typically 0.75 < P < 0.95 pu [39].

2.4 Inertia and the Swing Equation

This section discusses how the relationship between generator rotor inertia and the H-value that is commonly used in stability studies. This H-value will also be used in the new pole-slip protection function as is discussed in chapter 4.

Per definition, the inertia H-value of a machine is the kinetic energy stored in the rotor at rated speed divided by the machine apparent power (VA) rating:

$$H = \frac{\frac{1}{2} \cdot J \cdot \omega^2}{S_{VA}} \tag{2.1}$$

$$J = m \cdot R^2 = m \cdot \frac{D^2}{4} \tag{2.2}$$

where *J* is the machine inertia (kg.m^2)

m is the rotor mass (kg)

R is the rotor radius of gyration (m)

D is the rotor diameter of gyration (m)

ω is the rated speed (rad/s)

S_{VA} is the machine apparent power rating (VA)

The H-value can be expressed in metric units as follows:

$$\begin{aligned} H &= \frac{J \cdot \omega^2}{2 \cdot S_{VA}} \\ &= \frac{\frac{1}{2} \cdot J \cdot \left(n \cdot \frac{2\pi}{60} \right)^2}{S_{VA}} \\ &= \frac{5.4831 \times 10^{-3} J \cdot n^2}{S_{VA}} \\ &= \frac{5.4831 \times 10^{-9} J \cdot n^2}{S_{MVA}} \end{aligned} \tag{2.3}$$

where *n* is the rated speed (rpm)

S_{MVA} is the machine apparent power rating (MVA)

Larger machines will not necessarily have larger H-values. The H-value for round rotor synchronous machines (including the prime mover) is typically H = 3. Salient pole machines with their prime-movers has an H-value in the range of 6 < H < 10.

J can be calculated as follows from (2.1):

$$J = \frac{2 \cdot H \cdot S_{baseVA}}{\omega_{base}^2} \tag{2.4}$$

The acceleration of a machine can be calculated as follows:

$$T_m - T_e = \alpha \cdot J \tag{2.5}$$

where *J* is the inertia of the generator and prime-mover combined (kg.m^2)

From (2.4) and (2.5), the following expression is obtained:

$$
\begin{aligned}
&T_m - T_e = \frac{d\omega}{dt} \cdot \frac{2 \cdot H \cdot S_{baseVA}}{\omega_{base}^2} \\
&\frac{T_m - T_e}{2 \cdot H} = \frac{d\omega}{dt} \cdot \frac{T_{base}}{\omega_{base}} \\
&\frac{T_{m(p.u.)} - T_{e(p.u.)}}{2 \cdot H} \cdot \omega_{base} = \frac{d\omega}{dt} \\
&\int \left(\frac{T_{m(p.u.)} - T_{e(p.u.)}}{2 \cdot H} \cdot \omega_{base} \right) \cdot dt = \int d\omega \\
&\therefore \omega = \frac{\omega_{base}}{2H} \int \left(T_{m(p.u.)} - T_{e(p.u.)} \right) \cdot dt + \omega_o
\end{aligned}
\tag{2.6}
$$

where ω_o is the speed of the generator before the fault occurred

T_{base} is the rated torque of the generator

The rotor angle δ can be calculated as follows:

$$\delta = \int (\omega - \omega_0) \cdot dt \tag{2.7}$$

Equations (2.6) and (2.7) are presented in the block diagram shown in Figure 2.6.

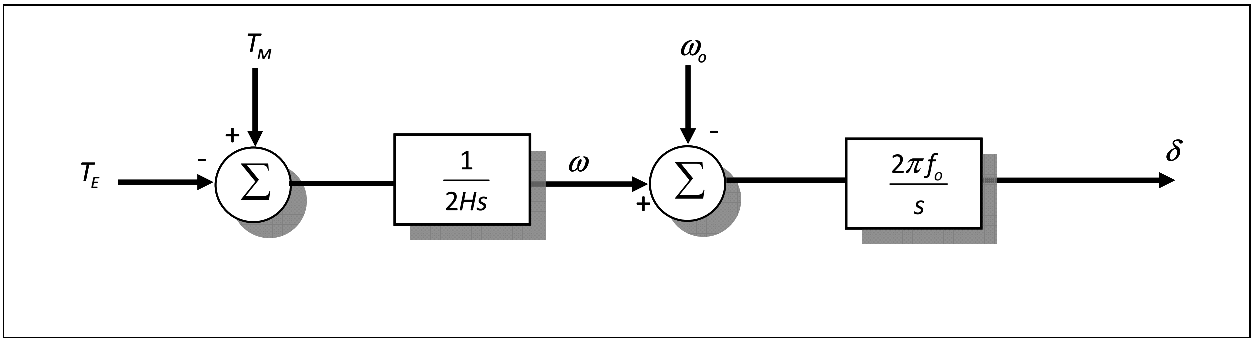

Figure 2.6: Diagram of swing equation [6:19]

The Koeberg nuclear power station in South Africa uses 1072 MVA, 1500 rpm generators with an H-value of 5.61 MWs/MVA [40]. The H-value means that the unloaded generator will accelerate from standstill to full speed in (2H) s if rated mechanical torque is applied to the generator rotor. In other words, the generator will accelerate from standstill to full speed in 5.61 x 2 = 11.22 s if rated torque is applied to the unloaded machine rotor. This is demonstrated by using equation (2.6) as follows:

$$\omega = \frac{\omega_{base}}{2H}\left(T_{m(p.u.)} - T_{e(p.u.)}\right)\cdot t$$

$$\omega = \frac{2\pi 50/2}{2\cdot 5.61}(1-0)\cdot(11.22\ \ s)$$

$$= 157.08\ \ rad.s^{-1}$$

$$\therefore n = 1500\ \ rpm$$

It should be noted that when equations (2.6) and (2.7) are used to determine the electrical power angle, the number of poles of the machine must be ignored by using $\omega_{base\_elec} = 2\pi f$. When the mechanical rotor angle or rotor speed is determined, the number of poles pairs (*p*) is important and $\omega_{base\_mech} = 2\pi f / p$.

2.5 Stability – Equal Area Criteria

The equal area criteria form an important part of the new pole slip protection function. This section provides an overview (which is expanded in more detail in chapter 4) of the equal area criteria.

The rotor motion of a generator is determined by Newton's second law (shown in section 2.4) as follows [30: 535]:

$$J\cdot\alpha_m(t) = T_m(t) - T_e(t) = T_a(t) \tag{2.8}$$

where T_a is the net accelerating torque [*N.m*]

$$\alpha_m(t) = \frac{d\omega_m(t)}{dt} = \frac{d^2\theta_m(t)}{dt^2} \tag{2.9}$$

where θ_m is the rotor angular position with respect to a stationary axis [rad]

It is convenient to express the mechanical angle of the rotor with respect to a synchronous rotating reference as follows:

$$\theta_m(t) = \omega_{msyn}\cdot t + \delta_m(t) \tag{2.10}$$

where ω_{msyn} is synchronous speed [rad/s]

δ_m is the rotor angular position with respect to a synchronously rotating reference [rad]

The electrical power angle $\delta_e(t)$ expressed in terms of $\delta_m(t)$:

$$\delta_e(t) = p\cdot\delta_m(t) \tag{2.11}$$

where *p* is the number of poles pairs of the generator

The electrical power delivered by a generator can be expressed as follows:

$$P_{elec} = \frac{|E| \cdot |V|}{X} \cdot \sin\delta \tag{2.12}$$

where X is the sum of the reactances of the generator and the power system

δ is the transfer angle

When the transfer angle is $\delta = \frac{\pi}{2}$ radians in equation (2.12), the power delivered by the generator will be a maximum. Figure 2.7 shows the electrical power versus transfer angle between the generator EMF and the network infinite bus. The constant mechanical power ($P_{mech} = P_0$) delivered by the turbine is also indicated on Figure 2.7.

At a time when the transfer angle is δ_0, a short-circuit occurs near the terminals of the generator and the electrical power falls to almost zero. The electrical power is nearly zero, since the faulted line has mainly reactive impedance. From equation (2.8), if the electrical torque is zero, and the mechanical torque remains positive, the rotor will accelerate. The transfer angle will accordingly increase from δ_0 to δ_c when the fault is cleared.

After the fault is cleared at $\delta = \delta_c$, the rotating mass will decelerate, but due to the inertia of the rotating mass, the power angle will reach a maximum value $\delta_{\max}$ somewhere between δ_c and δ_L. The generator will become unstable if the power angle increases to a value greater than δ_L. At $\delta = \delta_{\max}$, the rotor is rotating again at synchronous speed, but decelerates further due to the inertia of the rotating mass. Due to mechanical and electrical losses, the speed oscillations will be damped out so that the power angle stabilizes.

When Figure 2.7 is considered, the equal area criterion states that *Area 1* represents the increase in kinetic energy of the rotor (accelerating area) and *Area 2* represents the decrease in kinetic energy (decelerating area). Since the rotor must have the same speed (or kinetic energy) before a fault and after a fault, *Area 1* and *Area 2* must be equal to assure stability. If *Area 2* (deceleration area) is smaller than *Area 1* (acceleration area), the generator accelerates to the point that it becomes unstable.

If the fault is cleared later than is indicated on Figure 2.7, *Area 1* will be larger. *Area 2* must be equal to *Area 1* for the generator to remain stable. If it happens that the fault is cleared so late that $\delta_{\max}$ exceeds δ_L, the generator will become unstable. If $\delta_{\max}$ is greater than δ_L, P_{elec} will be less than P_{mech} and the generator will therefore accelerate to the point that it becomes unstable.

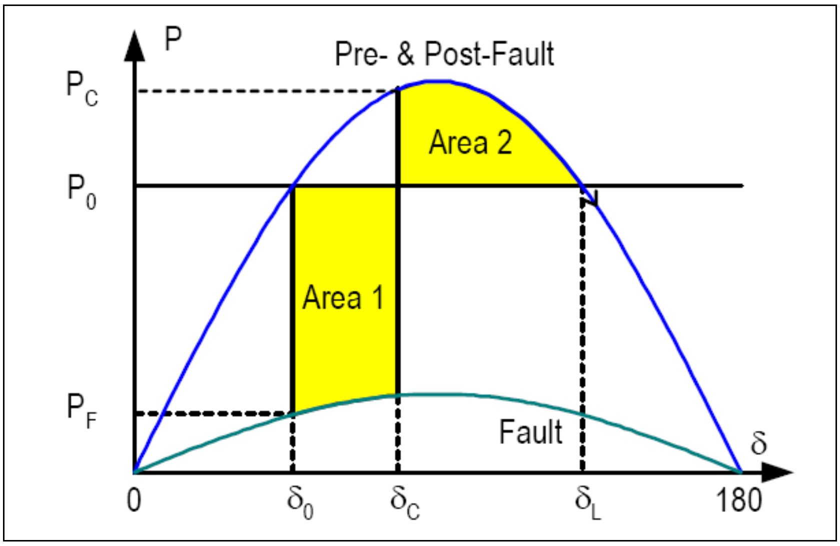

Figure 2.7: Measurement of stability by using equal area criterion [38]

The equal area criteria can be used to determine when a generator will pole-slip after a fault occurs in the network by considering δ as the transfer angle between the generator EMF and network infinite bus. The reactance X in equation (2.12) can be assumed to represent the generator transient direct-axis reactance $X_d^{'}$ plus the step-up transformer and transmission lines impedance to the infinite bus.

The generator EMF will remain fairly constant during the fault due to the large field time constant of synchronous machines. Once the pre-fault EMF is determined, this EMF can be used during fault conditions for up to 0.5 s after the fault started (see section 2.10).

The sinusoid equation $P_{\max} \cdot \sin\delta$ can be programmed into the pole-slip protection relay. The prime-mover mechanical power can be assumed to be the same as the generator electrical active power before the fault occurred. The accelerating area (Area 1) in Figure 2.7 can be calculated by considering the depth of the active power dip and the duration of the fault as follows [38]:

$$\begin{aligned} Area_1 &= \int_{\delta_0}^{\delta_c} \left(P_0 - P_{fault}\right) d\delta \\ &= P_0\left[\delta_c - \delta_0\right] - \int_{\delta_0}^{\delta_c} P_{fault}\, d\delta \end{aligned} \tag{2.13}$$

The decelerating area (Area 2) can be determined by calculating the area under the sinusoid minus the area $P_0\left[\delta_L - \delta_c\right]$ [38]:

$$\begin{aligned} Area_2 &= \int_{\delta_c}^{\delta_L} \left(\frac{E_{gen} \cdot V_{\inf}}{X_{total}} \cdot \sin\delta - P_0\right) d\delta \\ &= \left[-\frac{E_{gen} \cdot V_{\inf}}{X_{total}} \cos\delta - P_0 \cdot \delta\right]_{\delta_c}^{\delta_L} \\ &= \frac{E_{gen} \cdot V_{\inf}}{X_{total}}\left[\cos\delta_c - \cos\delta_L\right] - P_0\left[\delta_L - \delta_c\right] \end{aligned} \tag{2.14}$$

If *Area 1* becomes greater than *Area 2*, the machine must be tripped before the fault is cleared to avoid pole slipping and a possible damaging torque on the rotor.

2.6 MACHINE PARAMETERS

2.6.1 INTRODUCTION

This section gives an overview of how machine parameters are obtained and how the parameters should be used in simulations. Figure 2.8 shows simulated phase currents of a 120MVA, 13.8kV synchronous generator that was short-circuited from no-load at rated voltage (V_{rated}). The simulations were performed by using PSCAD. The machine terminals were short-circuited when the instantaneous value of the red phase voltage (I_a) was at a maximum. The short-circuit currents I_b and I_c contain a dc current component, while I_a has no dc component.

The following generator reactances were used in the PSCAD simulation:

$$X_d = 1.014 \text{ pu}$$

$$X_d^{'} = 0.314 \text{ pu}$$

$$X_d^{''} = 0.280 \text{ pu}$$

In order to explain the use and the calculation of machine parameters, the parameters will be determined from simulated short-circuit currents. The aim is to get the same generator parameter values, from the calculations to follow, as are given above. Since the short-circuit test is done from no-load, there will be no initial quadrature-axis component of flux [16]. The short-circuit current I_a in Figure 2.8 is described by the following expression [16]:

$$I_a = \frac{V}{X_{du}} + \left(\frac{V}{X_d^{'}} - \frac{V}{X_{du}}\right)e^{\frac{-t}{T_d^{'}}} + \left(\frac{V}{X_d^{''}} - \frac{V}{X_d^{'}}\right)e^{\frac{-t}{T_d^{''}}} \tag{2.15}$$

where V is the pre-fault terminal voltage

$\frac{V}{X_{du}}$ is the steady-state current component

$\left(\frac{V}{X_d^{'}} - \frac{V}{X_{du}}\right)e^{\frac{-t}{T_d^{'}}}$ is the transient current component

$\left(\frac{V}{X_d^{''}} - \frac{V}{X_d^{'}}\right)e^{\frac{-t}{T_d^{''}}}$ is the subtransient current component

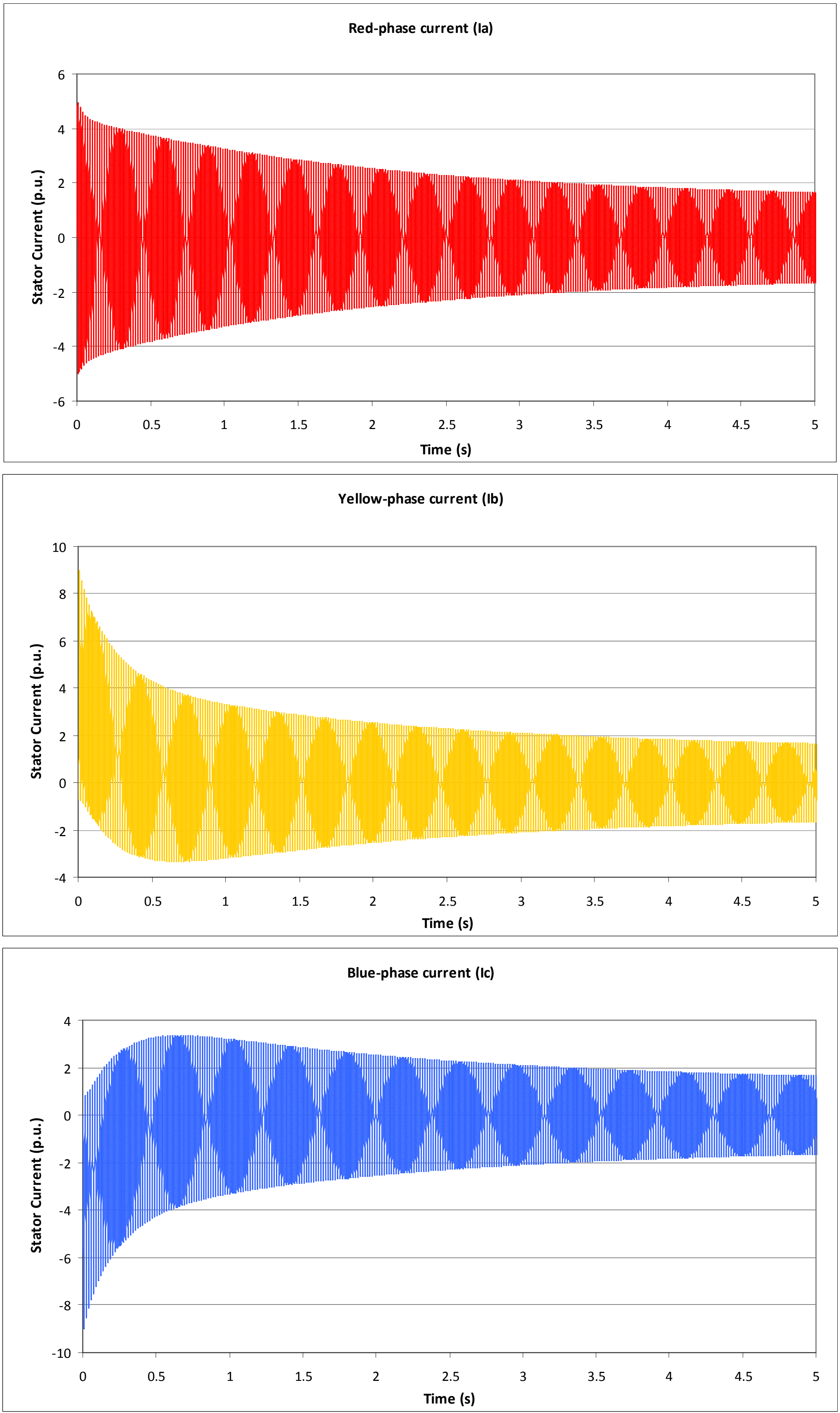

Figure 2.8: Synchronous machine short-circuit currents I_a, I_b and I_c

2.6.2 DETERMINATION OF X_d

This section describes a method that can be used to determine the direct axis reactance X_d of a synchronous machine.

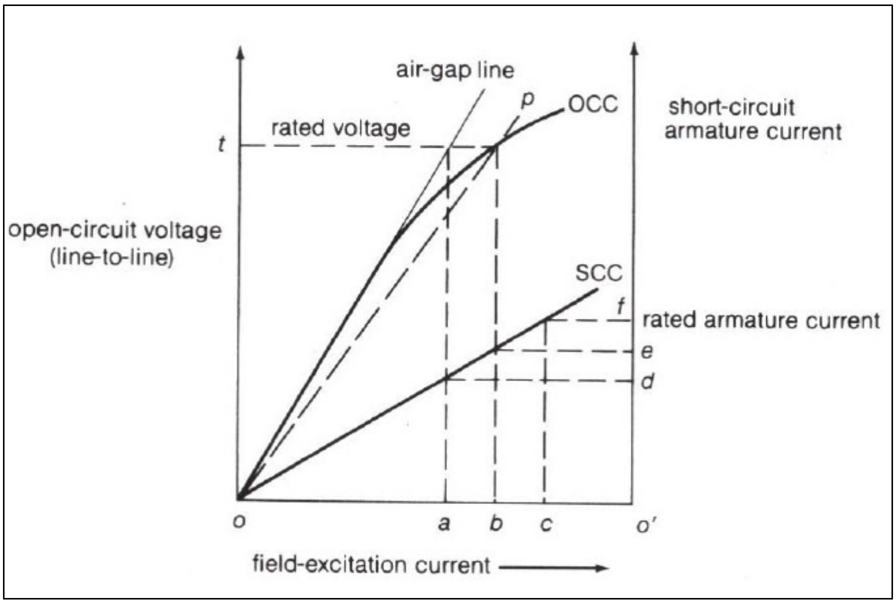

Figure 2.9: Synchronous machine open- and short-circuit characteristics [13:361]

Figure 2.9 shows the open and short-circuit characteristics of a synchronous machine. When the open and short-circuit characteristic curves for the generator are known, the unsaturated direct-axis reactance per phase can be determined as follows [13:361]:

$$X_d = \frac{ot}{\sqrt{3} \cdot o'd} \Omega / phase \tag{2.16}$$

The saturated direct-axis reactance per phase is determined as follows [13:361]:

$$X_{d(sat)} = \frac{ot}{\sqrt{3} \cdot o'e} \Omega / phase \tag{2.17}$$

The short-circuit ratio is defined [13:361]:

$$SCR = \frac{ob}{oc} \tag{2.18}$$

The synchronous machine open- and short-circuit characteristic curves of the simulated generator were not known. Instead, X_d can be calculated as follows:

$$X_d = \frac{V_{rated}}{I_{steady-state}} = \frac{1 \quad pu}{0.99 \quad pu} = 1.010 \quad pu \tag{2.19}$$

where $I_{steady-state}$ is the rms value of the steady-state component (at t = 5 s) of the red-phase current I_a in Figure 2.8.

It can be seen that the value of X_d as obtained from (2.19) corresponds well with the PSCAD simulated X_d value (1.014 pu).

2.6.3 DETERMINATION OF $X_d^{'}$

The subtransient time constant $T_d^{''}$ is typically small compared to the transient time constant $T_d^{'}$. The third term of equation (2.15) therefore becomes negligible after a few cycles. By subtracting the steady-state current from (2.15), the following expression is obtained [16]:

$$I - I_{steady\_state} = \left(\frac{V}{X_d^{'}} - \frac{V}{X_d} \right) e^{\frac{-t}{T_d^{'}}} \qquad (2.20)$$

Taking the natural logarithm of equation (2.20) gives:

$$\ln\left(I - I_{steady\_state}\right) = \ln\left(\frac{V}{X_d^{'}} - \frac{V}{X_d} \right)\left(\frac{-t}{T_d^{'}} \right) \qquad (2.21)$$

Equation (2.21) describes a straight line when plotted on a semi-log scale as is shown by the blue line in Figure 2.10. The red line in Figure 2.10 is the rms value of the short-circuited red-phase generator current that was presented in Figure 2.8.

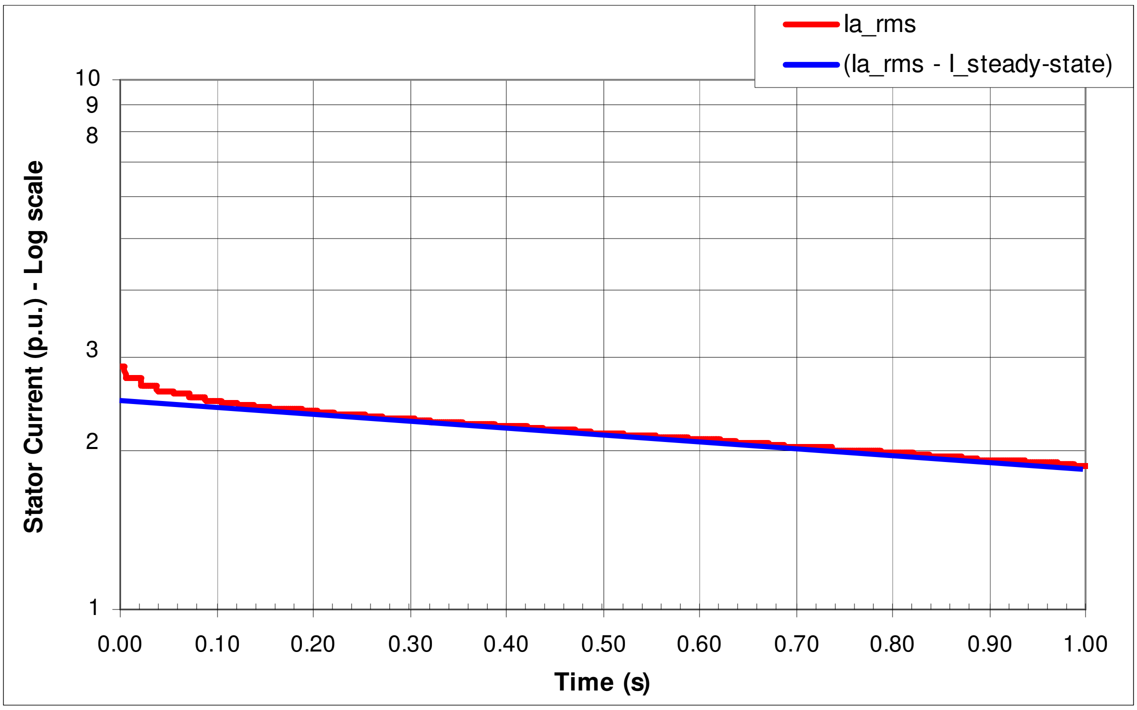

Figure 2.10: Synchronous machine short-circuit currents I_r,

The transient component of the current is obtained by extending the straight line back through the abscissa in Figure 2.10. The blue line intersects the vertical axis (t = 0 s) at a value of 2.37 pu. This value is the transient current $I_{transient}$.

The transient reactance $X_d^{'}$ can be calculated as follows [16]:

$$\frac{V_{rated}}{X_d^{'}} = I_{transient} + I_{steady\,state} \qquad (2.22)$$
$$= 2.37 + 0.99 = 3.36 \quad pu$$

$$\therefore X_d^{'} = \frac{1}{3.36} = 0.30 \quad pu \qquad (2.23)$$

It can be seen that the value of $X_d^{'}$ as obtained from (2.23) corresponds well with the PSCAD simulated $X_d^{'}$ value (0.314 pu).

2.6.4 DETERMINATION OF $X_d^{''}$

The following expression is true the instant that the three-phase fault is applied on the machine terminals (before the subtransient current become negligible) [16]:

$$I - I_{steady\_state} - I_{transient} = \left(\frac{V}{X_d^{''}} - \frac{V}{X_d^{'}} \right) e^{\frac{-t}{T_d^{''}}} \qquad (2.24)$$

Taking the natural logarithm of equation (2.24) gives:

$$\ln\left(I - I_{steady\_state} - I_{transient}\right) = \ln\left(\frac{V}{X_d^{''}} - \frac{V}{X_d^{'}} \right)\left(\frac{-t}{T_d^{''}} \right) \qquad (2.25)$$

The red curve in Figure 2.11 shows the synchronous generator rms current while the terminals are short-circuited. The aim is to determine the sub-transient reactance the instant when the fault is applied. This can be achieved by subtracting the blue curve from the red curve, which results in the green curve in Figure 2.11.

The subtransient current is represented by the green line and is calculated at time t = 0 as $I_{subtransient}$ = 2.71-2.37 = 0.34 pu.

The initial fault current (I_o) at t = 0 s is:

$$I_o = I_{steady\text{-}state} + I_{transient} + I_{subtransient} = 0.99+2.37+0.34 = 3.7 \text{ pu}$$

From equation (2.15) at t = 0, $I_0 = \frac{V_{rated}}{X_d^{''}}$.

$$\therefore X_d^{''} = \frac{V_{rated}}{I_0} = \frac{1}{3.7} = 0.270 \quad pu \qquad (2.26)$$

It can be seen that the value of $X_d^{''}$ as obtained from (2.26) corresponds well with the PSCAD simulated $X_d^{''}$ value (0.280 pu).

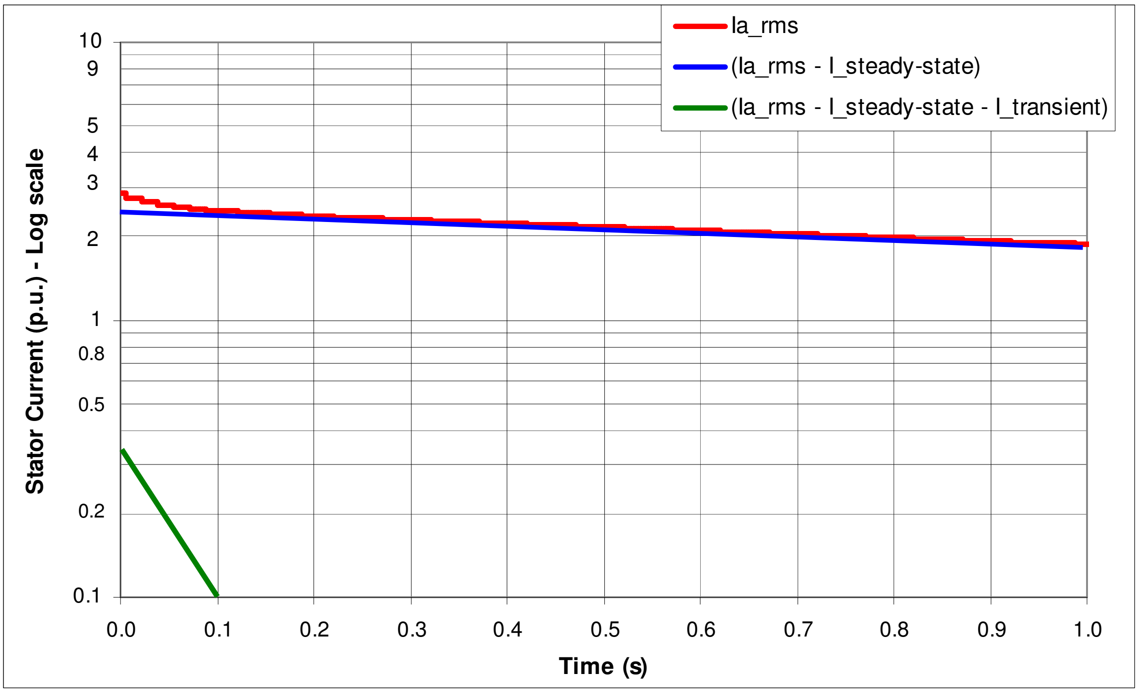

Figure 2.11: Synchronous machine short-circuit currents I_r,

2.6.5 DETERMINATION OF $T_d^{'}$

The direct-axis transient time constant $T_d^{'}$ can be found from the slope of the transient current (blue line) in Figure 2.10. The transient current will decrease from its initial value to e^{-1} (or 0.368) of its initial value in one time constant period [16:67]. In the simulation, the transient current decreases from 2.37 pu to 2.0 pu in 0.7 s.

$$\text{Therefore, } \frac{2.0}{2.37} = 0.844 = e^{\frac{-0.7}{T_d^{'}}}$$

$$\ln(0.844) = \frac{-0.7}{T_d^{'}}$$

$$\therefore T_d^{'} = \frac{-0.7}{\ln(0.844)} = 4.127 \text{ s}$$

The $T_d^{'}$ time constant determines the duration after a disturbance that the synchronous machine can be modelled as having a reactance of $X_d^{'}$.

2.6.6 DETERMINATION OF T_d''

The direct-axis subtransient time constant can be found from the slope of the subtransient current (green line) in Figure 2.11. In the simulation, the transient current decreases from its initial value of 0.34 pu to 0.1 pu in 0.1 s.

$$\text{Therefore, } \frac{0.1}{0.34} = 0.294 = e^{\frac{-0.1}{T_d''}}$$

$$\ln(0.294) = \frac{-0.1}{T_d''}$$

$$\therefore T_d'' = \frac{-0.1}{\ln(0.294)} = 0.082 \text{ s}$$

The T_d'' time constant determines the time after a disturbance in which the synchronous machine can be modelled to have a reactance of X_d''. Since the T_d'' time constant is very small, the machine will typically be modelled as having a reactance of X_d' during pole-slip conditions.

2.6.7 DETERMINATION OF X_q

The quadrature-axis reactance X_q can be calculated by using different methods. Some of these methods are given in reference [16]. This section will focus on the slip test method.

The slip test is conducted by driving the rotor at a speed slightly different from synchronous with the field open-circuited and the armature energized by a three-phase, rated frequency positive sequence power source. The voltage of the power source must be below the point on the open-circuit saturation curve where the curve deviates from the air-gap line. The corresponding armature current, armature voltage and the voltage across the open-circuit field winding are shown in Figure 2.12.

The unsaturated quadrature-axis reactance X_q can be obtained as follows [17:14]:

$$X_q = X_d \left(\frac{V_{\min}}{V_{\max}}\right)\left(\frac{I_{\min}}{I_{\max}}\right) \tag{2.27}$$

where V_{min} and V_{max} are the minimum and maximum values of the terminal voltage fluctuation respectively

I_{min} and I_{max} are the minimum and maximum values of the armature current fluctuation respectively

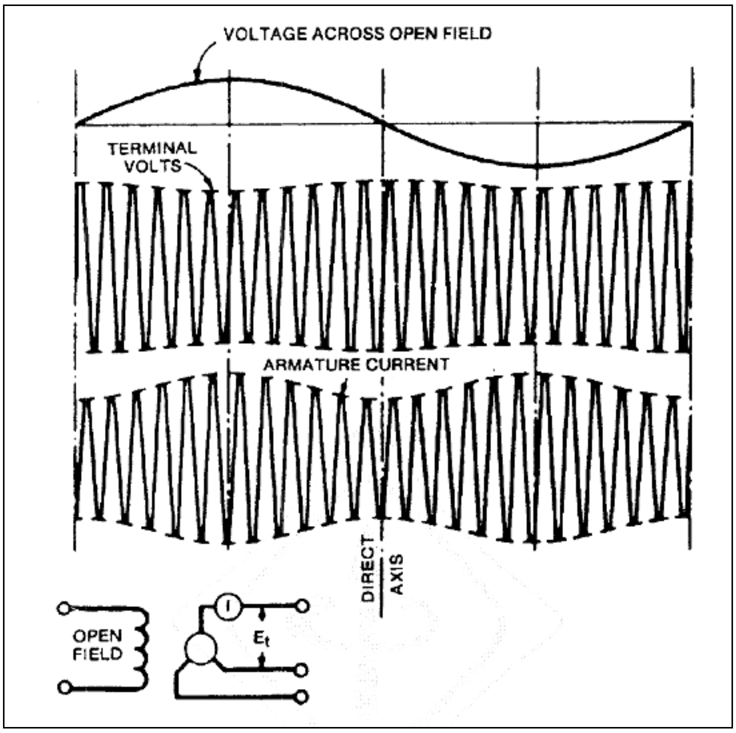

Figure 2.12: Slip-method used for obtaining Xq [17:13]

2.6.8 SYNCHRONOUS MACHINE MODELLING

This section discusses equivalent circuits that can be used to model synchronous machines. Both round rotor and salient pole machines have a degree of saliency, and must therefore both be modelled by using the d-axis and q-axis equivalent circuits.

The induced current paths in the rotor iron on the d- and q-axes change as the flux distributions change. This is especially true for solid cylindrical rotors, in which the tooth tops and slot wedges form a surface damper cage of relatively high resistance with a time constant typically less than 50 ms. As surface currents decay, lower resistance current paths in the poles and beneath the slots become effective, introducing higher reactances with time constants up to a few seconds. Hence the machine can be represented more accurately by having two damper windings on each axis [31:28/23].

In a salient pole rotor with laminated poles and specific damper cages, the damper circuits are more clearly defined (compared to solid iron poles), and a model with one damper on each axis (as well as the d-axis field) is accurate enough for many purposes [31:28/23]. Salient-pole generators with laminated rotors are usually constructed with copper-alloy damper bars located in the pole faces. These damper bars are often connected with continuous end-rings and thus, form a squirrel-cage damper circuit that is effective in both the direct axis and the quadrature axis. The damper circuit in each axis may then be represented by one circuit for salient pole machines [16].

Salient-pole machines with solid-iron poles may justify a more detailed model structure with two damper circuits in the d-axis, although the q-axis could still be modeled with one damper circuit [43],[44],[45]. For such a model, the parameters may have to be derived from tests such as the standstill frequency response tests, since salient pole data supplied by manufacturers is usually based on a Model 2.1 structure (one damper winding on the d-axis and q-axis respectively) as per the IEEE definition [16]. A model 2.2 structure is given in Figure 2.13 and Figure 2.14, which includes two damper circuits on the q-axis. The symbols in these figures are explained in the *List of Symbols* section.

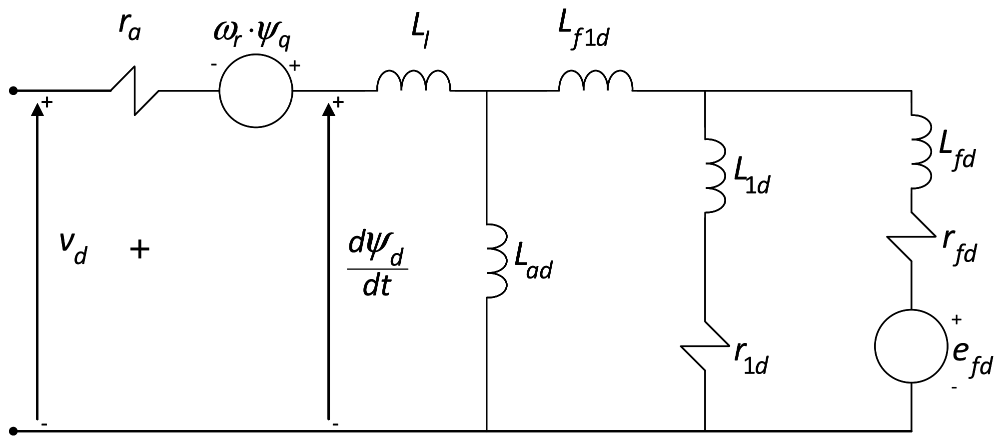

Figure 2.13: Synchronous machine d-axis equivalent circuit – reproduced from [15:89] and [16]

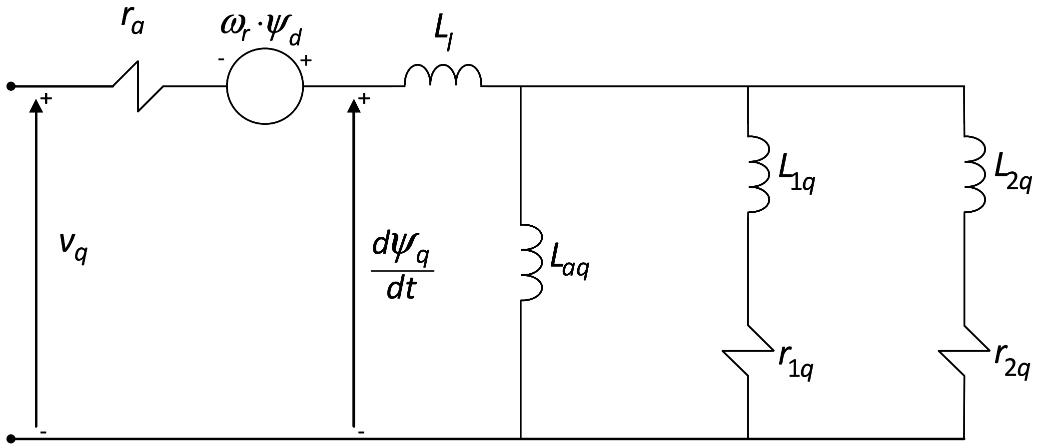

Figure 2.14: Synchronous machine q-axis equivalent circuit - reproduced from [15:89]

The voltages $\omega_r \cdot \psi_d$ and $\omega_r \cdot \psi_q$ represent the fact that a flux wave rotating in synchronism with the rotor will create voltages in the stationary armature coil and is referred to as *speed voltages*. The voltages $\frac{d\psi_d}{dt}$ and $\frac{d\psi_q}{dt}$ is referred to as *transformer voltages* and is only present during transient conditions.

The EMF of a synchronous generator is the open-circuit value of v_q. During *steady-state* conditions, the EMF E_q is simply the speed voltage:

$$E_q = \omega_r \cdot \psi_d \tag{2.28}$$

As explained earlier, salient-pole machines can be represented by only one damper winding in the q-axis circuit. That means L_{2q} and R_{2q} in Figure 2.15 can be ignored for salient pole machines. The series inductance L_{f1d} in the d-axis equivalent circuit represents the flux linking both the field winding and the damper winding, but not the stator winding [15:90]. It is common practice to neglect this series inductance since the flux linking the damper circuit is almost equal to the flux linking the armature winding [15:90]. This is so since the damper windings are near the air-gap. For short-pitched damper circuits and solid rotor iron paths, this approximation is not strictly valid [41]. There has been some emphasis on including the series inductance L_{f1d} for detailed studies [42]. Due to the complexity that results from the series inductance L_{f1d}, it will be neglected for illustration purposes in the sections to follow. By excluding the speed voltages and the series inductance L_{f1d}, the generator models can be represented as shown in the following figure.

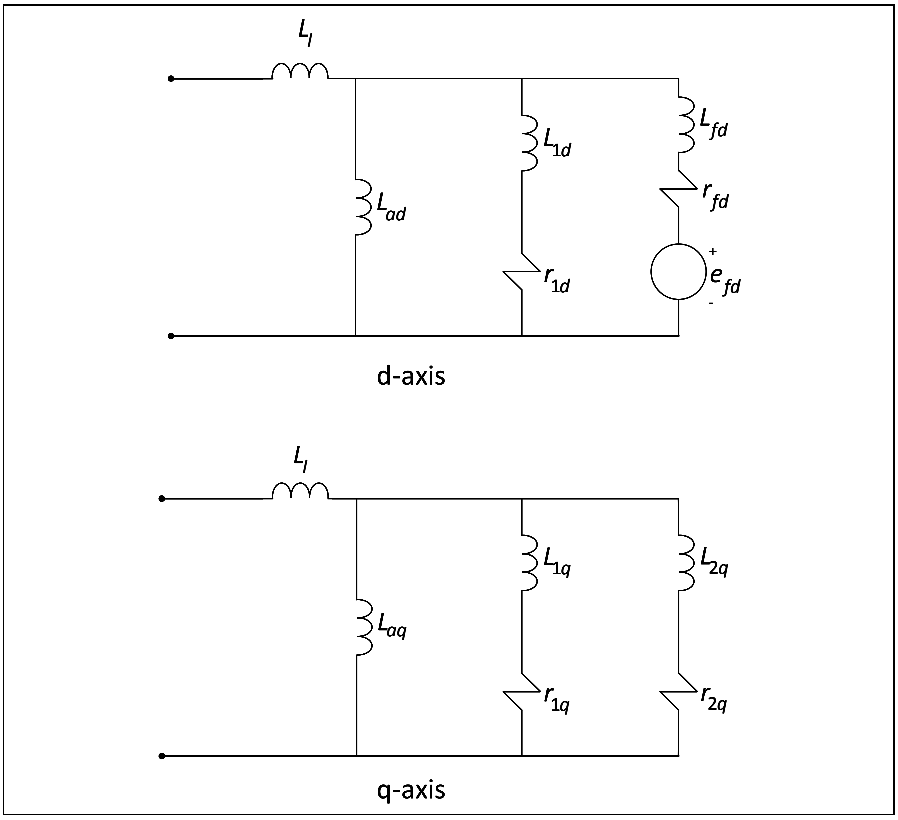

Figure 2.15: Synchronous machine q-axis equivalent circuit - reproduced from [31]

2.6.9 CONVERSION BETWEEN FUNDAMENTAL AND STANDARD PARAMETERS

Fundamental synchronous machine parameters are typically used in equivalent circuit models such as Figure 2.15, while standard machine parameters are normally available from synchronous machine manufacturer's data. This section describes the methods of converting fundamental parameters to standard parameters. The standard synchronous machine parameters are derived from Figure 2.15 by using the corresponding reactance values of the inductances ($X = 2\pi fL$).

2.6.9.1 Steady-state Reactances

During steady-state conditions, the field circuit and damper windings do not have an effect on the machine reactance. The steady-state reactances are determined from Figure 2.15 as follows [13:474]:

$$X_d = X_{ad} + X_l \tag{2.29}$$

$$X_q = X_{aq} + X_l \tag{2.30}$$

2.6.9.2 Transient Reactances

During transient conditions, the rotor field circuit in Figure 2.15 is included in the calculation of the direct-axis transient reactance, while the rotor damper winding is excluded [13:474].

$$X_d' = \frac{X_{ad} X_{fd}}{X_{ad} + X_{fd}} + X_l \tag{2.31}$$

The transient quadrature axis reactance X_q' for round rotor machines is calculated by including the first q-axis damper winding in Figure 2.15 [13:474]:

$$X_q' = \frac{X_{aq} X_{1q}}{X_{aq} + X_{1q}} + X_l \tag{2.32}$$

Salient pole machines are not modelled with a damper winding in transient conditions, hence the X_q' for salient pole machines is calculated as [13:474]:

$$X_q' = X_{aq} + X_l \tag{2.33}$$

From equations (2.30) and (2.33), it follows that $X_q = X_q'$ for salient pole machines. A new variable X_{q_avg} is introduced in section 4.7.4 to assist in using the equal area criteria (as part of the pole-slip function) to include the effect of saliency for round-rotor machines.

2.6.9.3 *Subtransient Reactances*

During subtransient conditions, the damper windings are included in the calculation of the subtransient reactances. The subtransient direct axis reactance of salient pole and round rotor machines is calculated from Figure 2.15 as follows [13:474]:

$$X_d^{''} = \frac{X_{ad}X_{fd}X_{1d}}{X_{ad}X_{fd} + X_{1d}X_{fd} + X_{1d}X_{ad}} + X_l \tag{2.34}$$

The subtransient quadrature axis reactance is [13:474]:

Round rotor machines:
$$X_q^{''} = \frac{X_{aq}X_{1q}X_{2q}}{X_{aq}X_{1q} + X_{aq}X_{2q} + X_{1q}X_{2q}} + X_l \tag{2.35}$$

Salient pole machines:
$$X_q^{''} = \frac{X_{aq}X_{1q}}{X_{aq} + X_{1q}} + X_l \tag{2.36}$$

2.6.9.4 *Time Constants*

The open circuit transient time constants $T_{do}^{'}$ and $T_{qo}^{'}$ is calculated as follows [13:474]:

Round rotor and salient pole:
$$T_{do}^{'} = \frac{1}{r_{fd}}\left[X_{ad} + X_{fd}\right] \tag{2.37}$$

Round rotor machines:
$$T_{qo}^{'} = \frac{1}{r_{1q}}\left[X_{aq} + X_{1q}\right] \tag{2.38}$$

Salient pole machines: $T_{qo}^{'}$ is not applicable

The $T_{do}^{'}$ time constant is larger with larger field leakage reactance X_{fd} and armature magnetizing reactance X_{ad}. The short-circuit transient direct-axis time constant $T_d^{'}$ is calculated as follows [13:474]:

$$T_d^{'} = \frac{1}{r_{fd}}\left[\frac{X_{ad}X_l}{X_{ad} + X_l} + X_{fd}\right] = \frac{X_d^{'}}{X_d}T_{do}^{'} \tag{2.39}$$

The $T_d^{'}$ time constant determines the duration after a disturbance when the synchronous machine can be modelled as having a reactance of $X_d^{'}$. $T_{do}^{'}$ is typically between 750 to 4000 radians (or 2 s and 11 s), and $T_d^{'}$ is typically a quarter of $T_{do}^{'}$ [13:471].

The open-circuit transient time constant $T_{do}^{'}$ determines how fast the field current can change when the excitation voltage is changed. Section 2.10 elaborates on how $T_{do}^{'}$ is used for excitation modelling.

The open-circuit sub-transient time constants are calculated as follows [13:474]:

$$T_{do}^{''} = \frac{1}{r_{1d}}\left[\frac{X_{ad}X_{fd}}{X_{ad}+X_{fd}}+X_{1d}\right] \tag{2.40}$$

Salient pole machines:
$$T_{qo}^{''} = \frac{1}{r_{1q}}\left[X_{aq}+X_{1q}\right] \tag{2.41}$$

Round rotor machines:
$$T_{qo}^{''} = \frac{1}{r_{2q}}\left[X_{2q}+\frac{X_{aq}X_{1q}}{X_{aq}+X_{1q}}\right] \tag{2.42}$$

The short-circuit sub-transient time constants are calculated as follows [13:474]:

$$T_{d}^{''} = \frac{1}{r_{1d}}\left[\frac{X_{ad}X_{fd}X_{l}}{X_{ad}X_{fd}+X_{fd}X_{l}+X_{ad}X_{l}}+X_{1d}\right]=\frac{X_{d}^{''}}{X_{d}^{'}}T_{do}^{''} \tag{2.43}$$

$$T_{q}^{''} = \frac{1}{r_{1q}}\left[\frac{X_{aq}X_{l}}{X_{aq}+X_{l}}+X_{1q}\right]=\frac{X_{q}^{''}}{X_{d}}T_{qo}^{''} \tag{2.44}$$

Note that all the time constants expressed in this section have units of radians. All the time constants must be divided by $\omega = 2\pi f$ (rad/s) to give results in units of seconds.

2.7 EFFECT OF SALIENCY

Both salient pole machines and round rotor machines have some degree of saliency. Round rotor machines have some degree of saliency, since the round rotor windings are not distributed evenly. This causes a greater flux path reluctance on the quadrature axis, which has the effect that the quadrature-axis reactance is lower than the direct-axis reactance.

The following equations give the basic relations between EMF (*E*), flux (ϕ), current (*I*), inductance (*L*), reactance (*X*), number of winding turns (*N*) and reluctance ($\Re$) [4]:

$$\begin{aligned}\phi &= \frac{Ni}{\Re}\\ E &= -\frac{d\phi}{dt}\\ L &= \frac{N\phi}{i}\\ X &= 2\pi f L\end{aligned} \tag{2.45}$$

When saliency is neglected, the machine fluxes are assumed to be distributed evenly around the periphery of the machine. The resultant air-gap flux ($\overline{\phi_r}$) can be considered as the phasor sum of the field flux ($\overline{\phi_f}$) and armature reaction flux ($\overline{\phi_{ar}}$) as is shown in Figure 2.16.

The fluxes $\overline{\phi_f}$ and $\overline{\phi_{ar}}$ are respectively produced by the field and armature reaction MMFs, which are caused by the field and armature currents, respectively. The fluxes manifest themselves into voltages 90^o out-of-phase with the fluxes. It can also be seen from Figure 2.16 that the armature reaction flux $\overline{\phi_{ar}}$ is in-phase with the line current $\overline{I_a}$ producing it. The armature reaction EMF $\overline{E_{ar}}$ lags $\overline{\phi_{ar}}$ and $\overline{I_a}$ by 90^o.

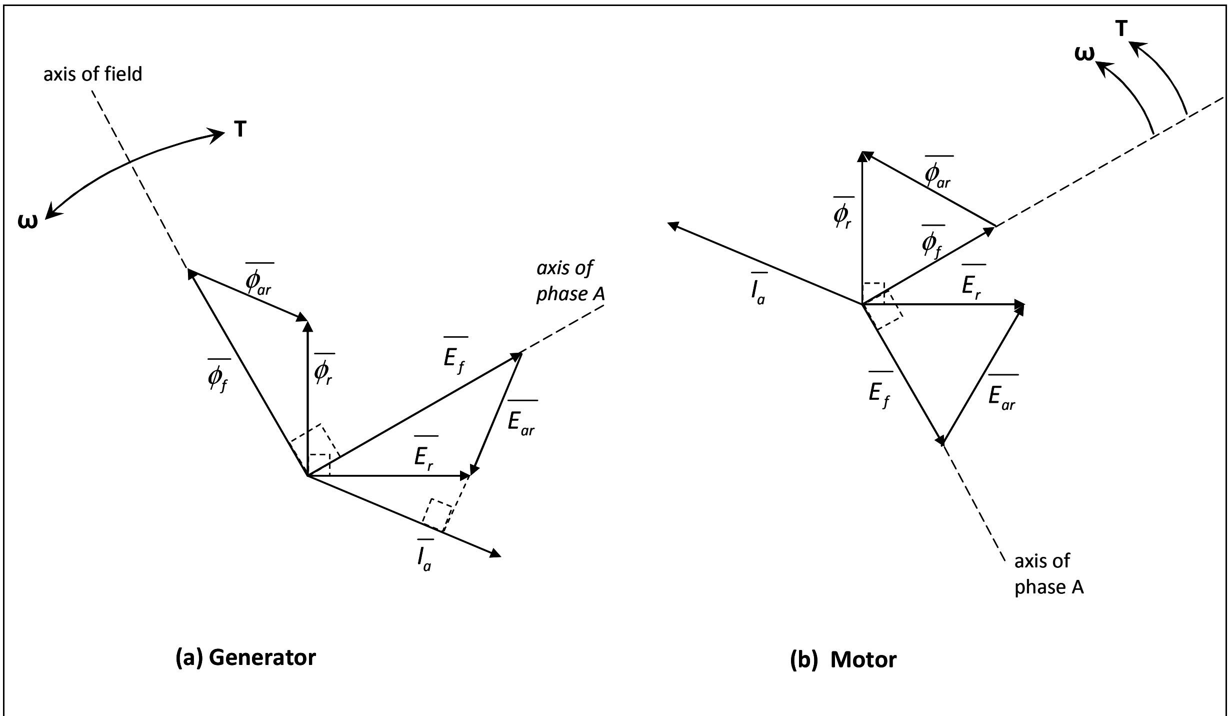

Figure 2.16: Relationship between fluxes, voltages and currents in a round rotor synchronous machine – reproduced from [13:355]

$\overline{E_{ar}}$ and $\overline{E_f}$ are proportional to the armature and field currents respectively. The effect of armature reaction can be considered to be that of inductive reactance (X_ϕ). This reactance is known as the *magnetizing reactance* or *armature-reaction reactance* and is indicated in Figure 2.17.

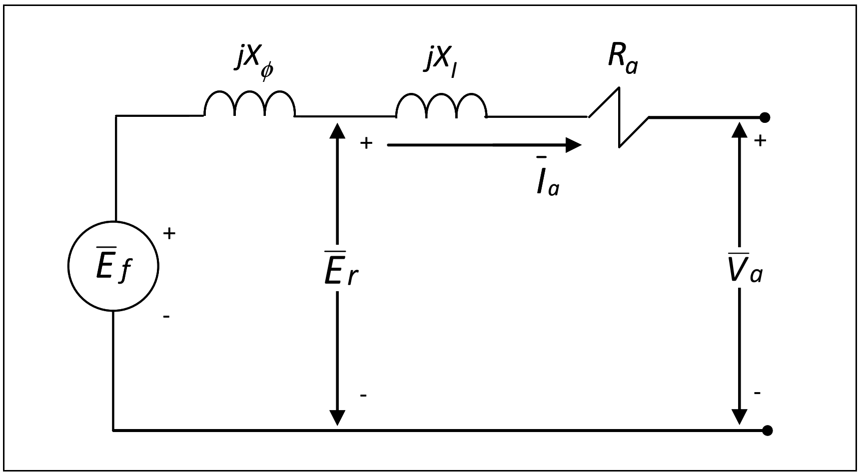

Figure 2.17: Per phase equivalent circuit of a round rotor synchronous machine [13:356]

The relationship between the EMF vectors is indicated in equation (2.46).

$$\bar{E}_r = \bar{E}_f + \bar{E}_{ar} = \bar{E}_f - j\bar{I}_a X_\phi \tag{2.46}$$

The terminal voltage ($\bar{V}_a$) of a synchronous generator can be expressed as follows:

$$\begin{aligned}\bar{V}_a &= \bar{E}_f - \bar{I}_a R_a - j\bar{I}_a\left(X_l + X_\phi\right)\\ &= \bar{E}_f - \bar{I}_a R_a - j\bar{I}_a X_s\end{aligned} \tag{2.47}$$

where X_l is the stator leakage reactance

$X_s = X_l + X_\phi$ is the synchronous reactance

The effects of saliency are taken into account by the two-reactance theory proposed by Blondel [32] and extended by Doherty, Nickle [33], Park [34] and others. The armature current $\bar{I}_a$ is resolved into two components, I_q in-phase with the excitation EMF ($\bar{E}_f$) and I_d 90° out-of-phase with $\bar{E}_f$, as shown in Figure 2.18.

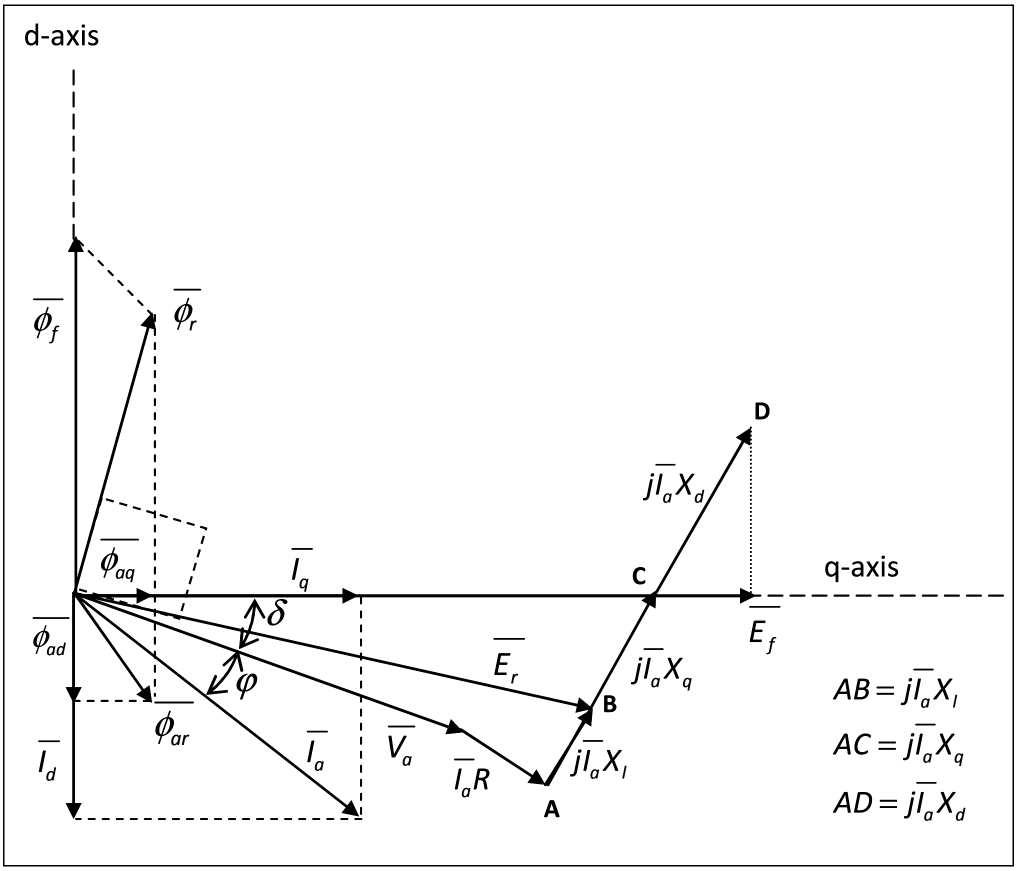

Figure 2.18: Steady-state phasor diagrams for a salient pole synchronous machine – reproduced from [13:379]

The currents I_d and I_q produce armature reaction fluxes ϕ_{ad} and ϕ_{aq} respectively. The resultant armature reaction flux is given as:

$$\overline{\phi}_{ar} = \phi_{aq} + j\phi_{ad} \tag{2.48}$$

It can be seen from Figure 2.16 that $\overline{\phi_{ar}}$ is in-phase with $\overline{I_a}$ for a round rotor. Due to the higher reluctance on the quadrature-axis of a salient pole rotor, $\overline{\phi_{ar}}$ will have a component $\overline{\phi}_{aq}$ that is smaller than $\overline{\phi}_{ad}$. For this reason $\overline{\phi_{ar}}$ will not be in-phase with $\overline{I_a}$ for a machine with saliency. Due to saliency, it is not possible to describe the voltage drop reactance between the EMF and terminal voltage with a single reactance.

When machine stability is predicted, the magnitude of the EMF on the positive q-axis will have a significant effect on how stable the machine is. The machine has a better stability when the magnitude of the EMF on the positive q-axis is higher. It must be noted that the fluxes cannot change instantaneously during a fault on the generator terminals.

Once a fault appears on the generator terminals, the exciter will increase the excitation voltage. Due to a high field circuit inductance, the field current will not increase instantaneously. The EMF E_f will increase linearly with the field current during unsaturated conditions. Section 2.10 provides more detail regarding excitation systems and machine stability.

A salient pole machine is "stiffer" or more stable than a round-rotor machine. This can be explained by investigating the vector diagram in Figure 2.21 in section 2.8. When X_q is smaller than X_d, the product of $j\overline{I_q}X_q$ will also be smaller for the same EMF voltage. This means that $\overline{V_d}$ will be smaller (when R_a is neglected) and therefore resulting in a smaller power angle δ. Although $\overline{I_q}$ increases with a decreasing X_q, the product $j\overline{I_q}X_q$ is still smaller with a smaller X_q.

Figure 2.19 and Figure 2.20 show the relationship between active electrical power and the power angle of a synchronous machine during steady-state and transient conditions respectively. Saliency will cause a second order harmonic power frequency as indicated in Figure 2.19 and Figure 2.20. The resultant power output vs. power angle curve indicates that the maximum possible active power output is greater when saliency is present.

The transient power relationship in Figure 2.20 is only valid for salient pole machines, and not for round rotor machines. Salient pole synchronous machines are modelled with a quadrature axis reactance X_q that is equal to the transient quadrature reactance $X_q^{'}$. For that reason X_q (instead of $X_q^{'}$) can be used to determine the salient component of active power during transient conditions for salient pole machines. Round rotor machines have an $X_q^{'}$ that is different to X_q, which means X_q cannot be used to determine the salient component of active power during transient conditions. As part of the new pole-slip function, a method must be developed that can predict what the value of the quadrature axis reactance (X_{q_avg}) will be for round rotor machines after a network disturbance (refer to section 4.7.4).

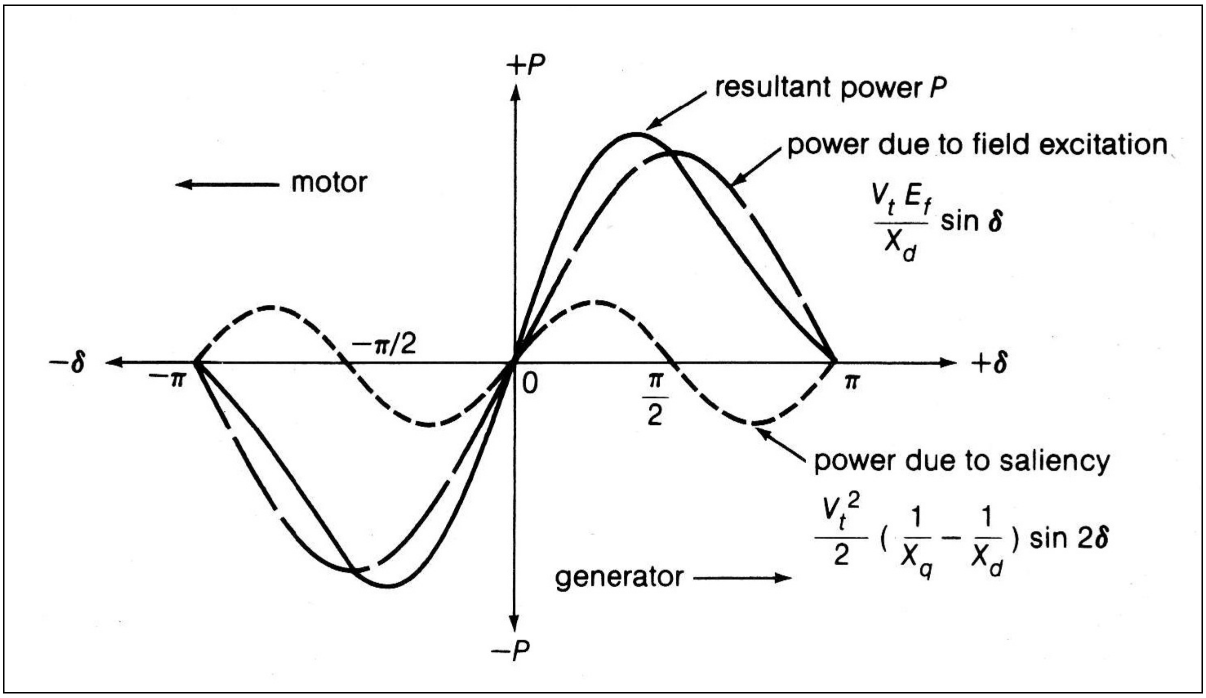

Figure 2.19: Steady-state power angle relationship of a synchronous machine [13:380]

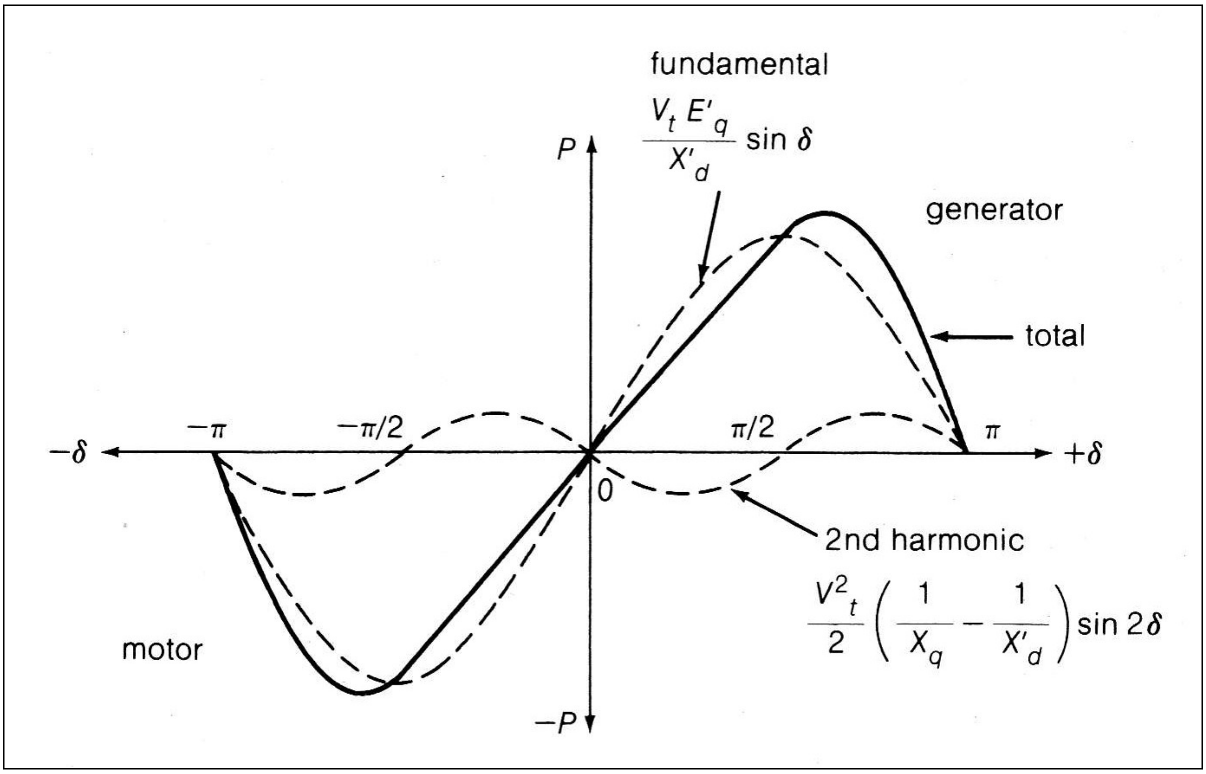

Figure 2.20: Transient power angle relationship of a synchronous machine [13:482]

2.8 POWER ANGLE CALCULATION

One of the criteria of the new pole-slip protection function will be to make decisions based on the machine power angle. Chapter 4 gives more detail on how the power angle will be incorporated in the new pole-slip protection function. The synchronous machine phasor diagrams need to be understood in order to find an algorithm that can be programmed into the relay to calculate the power angle in real time.

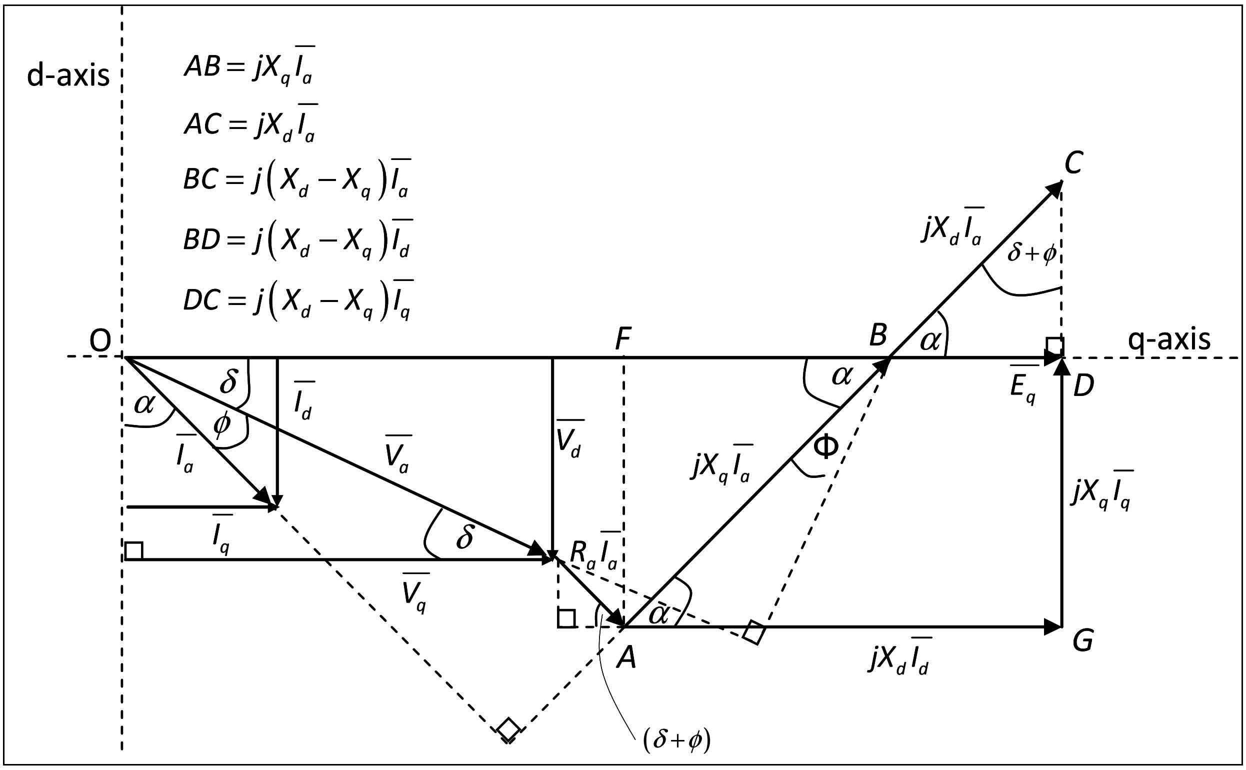

Figure 2.21: Phasor diagram for an overexcited generator (generator convention)

Figure 2.21 shows the phasor diagram of an overexcited generator. The machine excitation voltage or steady-state EMF ($\overline{E_q}$) is located on the quadrature-axis and is represented by phasor OD:

$$\overline{E_q} = \overline{V_a} + \overline{I_a}R_a + j\overline{I_d}X_d + j\overline{I_q}X_q \tag{2.49}$$

The only measurable quantities available to the pole-slip relay are the terminal voltage $\overline{V_a}$, the line current $\overline{I_a}$ and the associated power factor angle Φ. An algorithm must therefore be developed that makes use of only the above-mentioned quantities in order to calculate the power angle δ. For large machines, the armature resistance R_a can be neglected, but the resistance is included in the phasor diagram.

The voltage and current phasors are drawn in their d- and q-axis components and is defined as follows:

$$
\begin{aligned}
\overline{I_d} &= \overline{I_a}\sin(\delta+\phi) \\
\overline{I_q} &= \overline{I_a}\cos(\delta+\phi) \\
\overline{V_q} &= \overline{V_a}\cos\delta \\
\overline{V_d} &= j\overline{I_q}X_q - \overline{I_a}R_a\sin(\delta+\phi) \\
&= j\overline{I_a}X_q\cos(\delta+\phi) - \overline{I_a}R_a\sin(\delta+\phi)
\end{aligned}
\tag{2.50}
$$

The following trigonometric identities are used in the derivation below:

$$
\begin{aligned}
\cos(\alpha+\beta) &= \cos\alpha\cos\beta - \sin\alpha\sin\beta \\
\sin(\alpha+\beta) &= \sin\alpha\cos\beta + \cos\alpha\sin\beta
\end{aligned}
\tag{2.51}
$$

$$
\frac{\sin\alpha}{\cos\alpha} = \tan\alpha \tag{2.52}
$$

From the phasor diagram, the power angle δ can be determined from:

$$
\tan\delta = \frac{|V_d|}{|V_q|} \tag{2.53}
$$

From equations (2.50) and (2.53):

$$
\tan\delta = \frac{|V_d|}{|V_q|} = \frac{|I_a|X_q\cos(\delta+\phi) - |I_a|R_a\sin(\delta+\phi)}{|V_a|\cos\delta} \tag{2.54}
$$

By using the trigonometric identities of (2.51) in (2.54) it follows:

$$
\begin{aligned}
\tan\delta &= \frac{|I_a|X_q(\cos\delta\cos\phi - \sin\delta\sin\phi) - |I_a|R_a(\sin\delta\cos\phi + \cos\delta\sin\phi)}{|V_a|\cos\delta} \\
&= \frac{|I_a|X_q}{|V_a|}\cos\phi - \frac{|I_a|X_q}{|V_a|}\left(\frac{\sin\delta}{\cos\delta}\right)\sin\phi - \frac{|I_a|R_a}{|V_a|}\left(\frac{\sin\delta}{\cos\delta}\right)\cos\phi - \frac{|I_a|R_a}{|V_a|}\sin\phi
\end{aligned}
\tag{2.55}
$$

By using the trigonometric identity of (2.52) in (2.55) it gives:

$$
\tan\delta = \frac{|I_a|X_q}{|V_a|}\cos\phi - \frac{|I_a|X_q}{|V_a|}\tan\delta\sin\phi - \frac{|I_a|R_a}{|V_a|}\tan\delta\cos\phi - \frac{|I_a|R_a}{|V_a|}\sin\phi \tag{2.56}
$$

Re-arranging the tan δ terms gives:

$$
\tan\delta\left(1 + \frac{|I_a|X_q}{|V_a|}\sin\phi + \frac{|I_a|R_a}{|V_a|}\cos\phi\right) = \frac{|I_a|X_q}{|V_a|}\cos\phi - \frac{|I_a|R_a}{|V_a|}\sin\phi \tag{2.57}
$$

$$
\therefore \tan\delta\left(\frac{|V_a| + |I_a|X_q\sin\phi + |I_a|R_a\cos\phi}{|V_a|}\right) = \frac{|I_a|X_q\cos\phi - |I_a|R_a\sin\phi}{|V_a|} \tag{2.58}
$$

$$
\therefore \tan\delta = \left(\frac{|I_a|X_q\cos\phi - |I_a|R_a\sin\phi}{|V_a| + |I_a|X_q\sin\phi + |I_a|R_a\cos\phi}\right) \tag{2.59}
$$

By taking the arc tan of equation (2.59), the power angle δ can be calculated as:

$$\therefore \delta = \tan^{-1}\left(\frac{|I_a|X_q\cos\phi - |I_a|R_a\sin\phi}{|V_a| + |I_a|X_q\sin\phi + |I_a|R_a\cos\phi}\right) \tag{2.60}$$

By neglecting the armature resistance R_a, equation (2.60) simplifies to:

$$\therefore \delta = \tan^{-1}\left(\frac{|I_a|X_q\cos\phi}{|V_a| + |I_a|X_q\sin\phi}\right) \tag{2.61}$$

Equation (2.61) can easily be implemented into a pole-slip protection relay, since the magnitudes V_a, I_a and Φ can be measured, and X_q can be obtained from the synchronous machine datasheets. It will be shown in chapter 4 that this equation will only be used as part of the steady state transfer angle calculations in the new pole-slip function. Since this expression will not be used for transient conditions, the non-linearity of the tangent function around 90° is not a problem, since the steady-state (pre-fault) generator power angle will be well below 90°.

The triangle BCD of Figure 2.21 will collapse in the case of a round rotor machine (with no saliency). In the case of no saliency, the phasor AD could be drawn as a vector $jX_d\overline{I_a}$. The phasor diagram for a round rotor machine with no saliency is described as follows:

$$\overline{E_q} = \overline{V_a} + \overline{I_a}R_a + j\overline{I_a}X_d \tag{2.62}$$

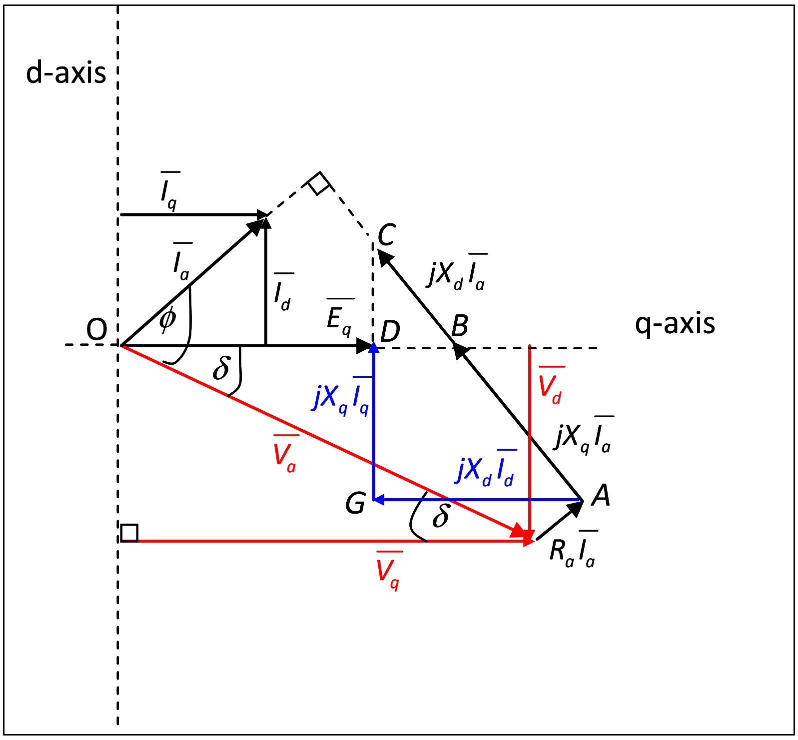

Figure 2.22: Phasor diagram for an underexcited generator (generator convention)

The phasor diagram of an underexcited generator is shown in Figure 2.22. It can be shown that the power angle for an *underexcited* generator is calculated as follows:

$$\delta = \tan^{-1}\left(\frac{I_a X_q \cos\phi}{V_a - I_a X_q \sin\phi}\right) \tag{2.63}$$

The only difference between equations (2.61) and (2.63) is the sign in the denominator. These two equations are valid for generating- and motoring mode. In summary, Table 2.1 gives the equations for the calculation of the power angle for the different synchronous machine operating states.

Table 2.1: Algorithms for the calculation of power angle (armature resistance neglected)

	Underexcited	***Overexcited***
Generating mode	$\delta = \tan^{-1}\left(\frac{I_a X_q \cos\phi}{V_a - I_a X_q \sin\phi}\right)$	$\delta = \tan^{-1}\left(\frac{I_a X_q \cos\phi}{V_a + I_a X_q \sin\phi}\right)$
Motoring mode	$\delta = \tan^{-1}\left(\frac{I_a X_q \cos\phi}{V_a - I_a X_q \sin\phi}\right)$	$\delta = \tan^{-1}\left(\frac{I_a X_q \cos\phi}{V_a + I_a X_q \sin\phi}\right)$

2.9 PRIME MOVER TRANSIENT BEHAVIOUR

When an electrical fault occurs near a generator, the electrical active power delivered by the generator reduces, while the reactive power increases. The mechanical prime mover torque will be greater than the electrical active power (torque) during the fault, which will cause the generator to speed up.

A generator governor system can be set into one of two modes, namely speed control or power control [49]. The governor can be used to keep the generator speed (frequency) at the rated value (normally in islanded situations), or the governor can be used to keep the generator electrical active power output load at a specific value [15:426]. When the generator speed needs to increase, a steam valve must be opened to allow more steam into the prime mover turbines.

Governor systems for fossil-fuelled and nuclear power stations have a large overall time constant, which means that when the steam control valve position changes, the prime mover torque on the generator shaft will not increase immediately [15:426]. Due to the large time constant, the steady-state mechanical power output of a steam turbine can remain near constant for as long as 300 ms to 500 ms while an electrical fault is on the system. This will cause the generator speed to increase approximately linearly with time during the electrical fault. The new pole-slip protection function can therefore assume constant prime mover torque during the fault.

2.10 EXCITATION SYSTEM TRANSIENT BEHAVIOUR

The excitation system of a generator will immediately react on a fault close to the generator by increasing the excitation voltage E_{fd}. Due to the large field leakage reactance X_{fd} (or the resulting field time constant) the field current I_{fd} will not change instantaneously with a larger E_{fd} (refer to section 4.7.3).

Figure 2.23 gives a synchronous machine block diagram with subtransient effects neglected and with a simplified excitation system included. A Matlab simulation of this generator model is shown in Figure 2.24 with the following parameters:

$$X_d = 1.81 \quad pu$$
$$X_d^{'} = 0.3 \quad pu$$
$$T_{do}^{'} = 8 \quad s$$

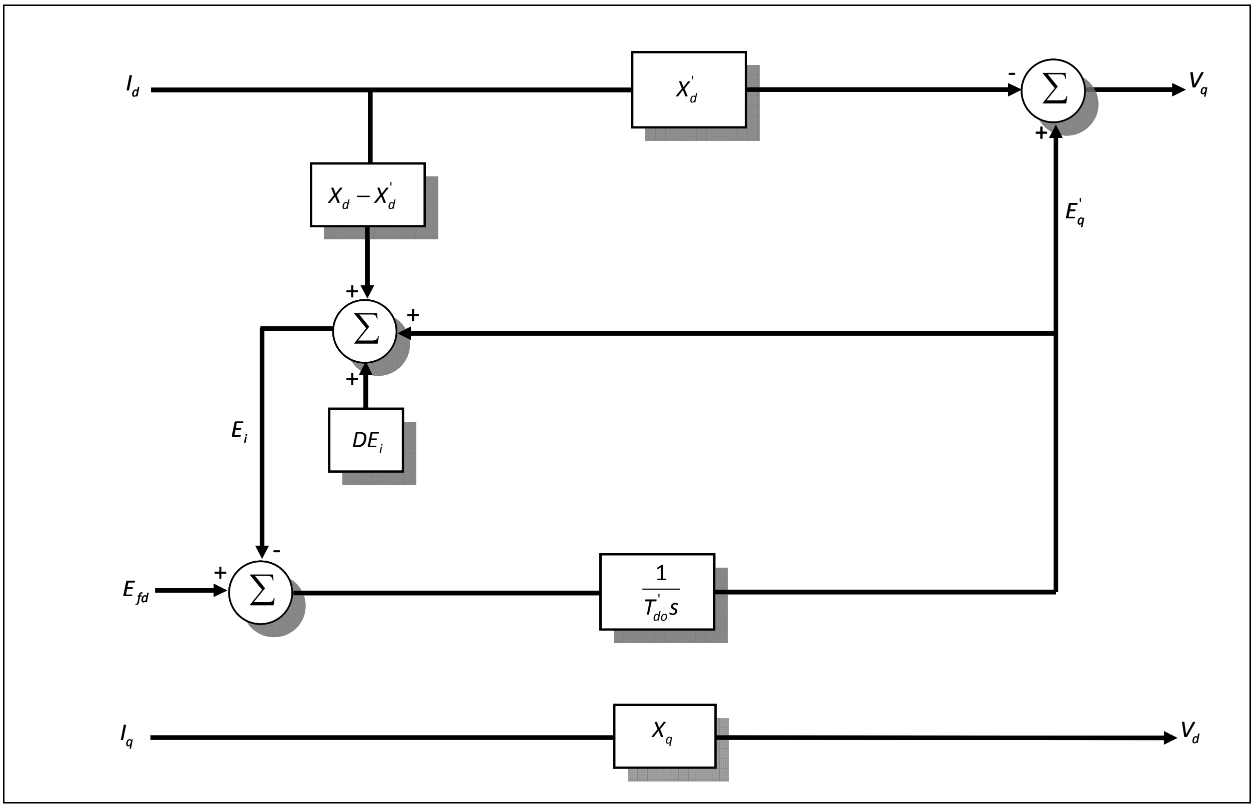

Figure 2.23: Salient pole synchronous machine model (subtransient effects neglected) - reproduced from [6]

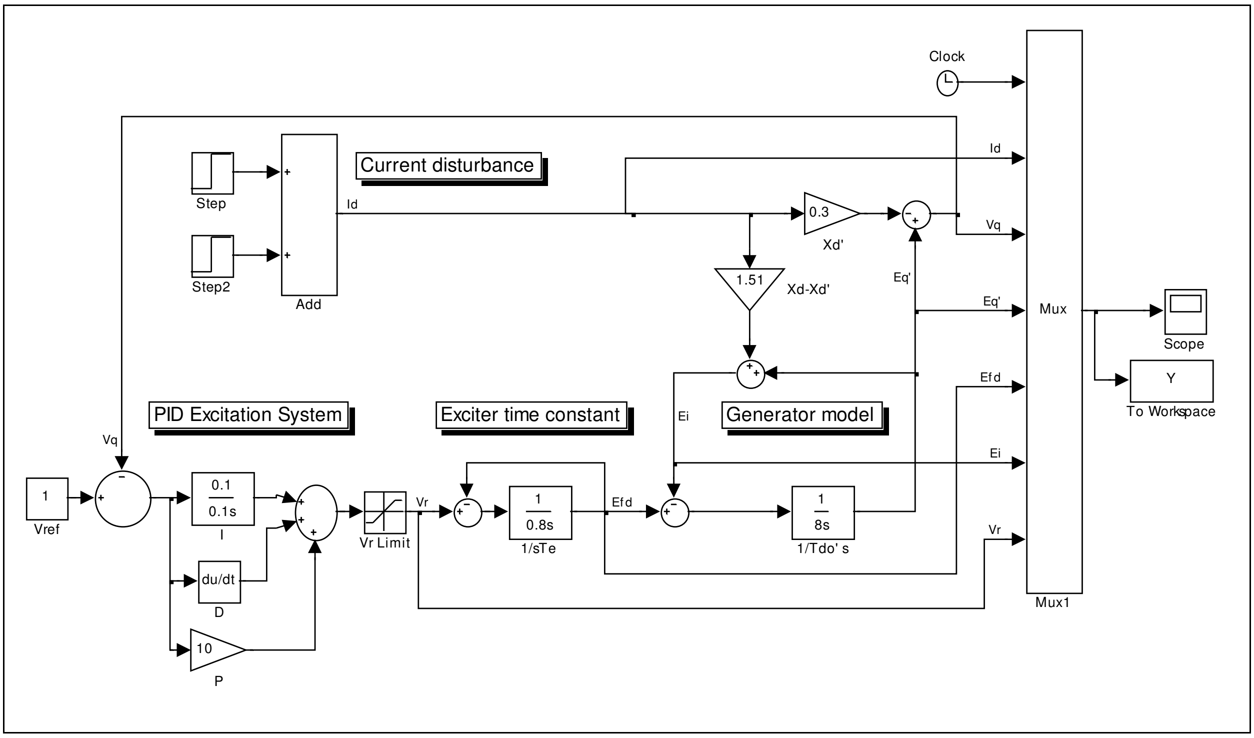

Figure 2.24: MATLAB simulation diagram of a synchronous machine with EMF indicated

Figure 2.25 provides the results of a simulation that was performed on the model shown in Figure 2.24. The generator transient EMF $E_q^{'}$ is plotted against the main exciter excitation voltage E_{fd}. The main rotating exciter (of a brushless exciter) can have a field time constant of typically 0.5 s to 2 s. This causes the lag between the excitation regulator voltage V_r and the main exciter voltage E_{fd}. Due to the large field time constant of the generator ($T_{do}^{'}$ = 8 s in this example), $E_q^{'}$ remains almost constant during the simulation time.

It should be noted that E_{fd} could increase faster than what is indicated in Figure 2.25 when an exciter other than a rotating exciter is used. The rotating exciter has a considerable time constant due to the rotating main exciter inductance.

When saliency is neglected, V_q and I_d in Figure 2.23 can be regarded as the generator terminal voltage and line current. When E_i (from Figure 2.23) is greater than E_{fd} during a fault, the transient EMF $E_q^{'}$ will reduce as can be seen in Figure 2.25. In this simulation, $E_q^{'}$ would only increase during the fault if the fault current was smaller. It can therefore be concluded that the transient EMF $E_q^{'}$ can decrease during a fault even if the excitation system reacts rapidly.

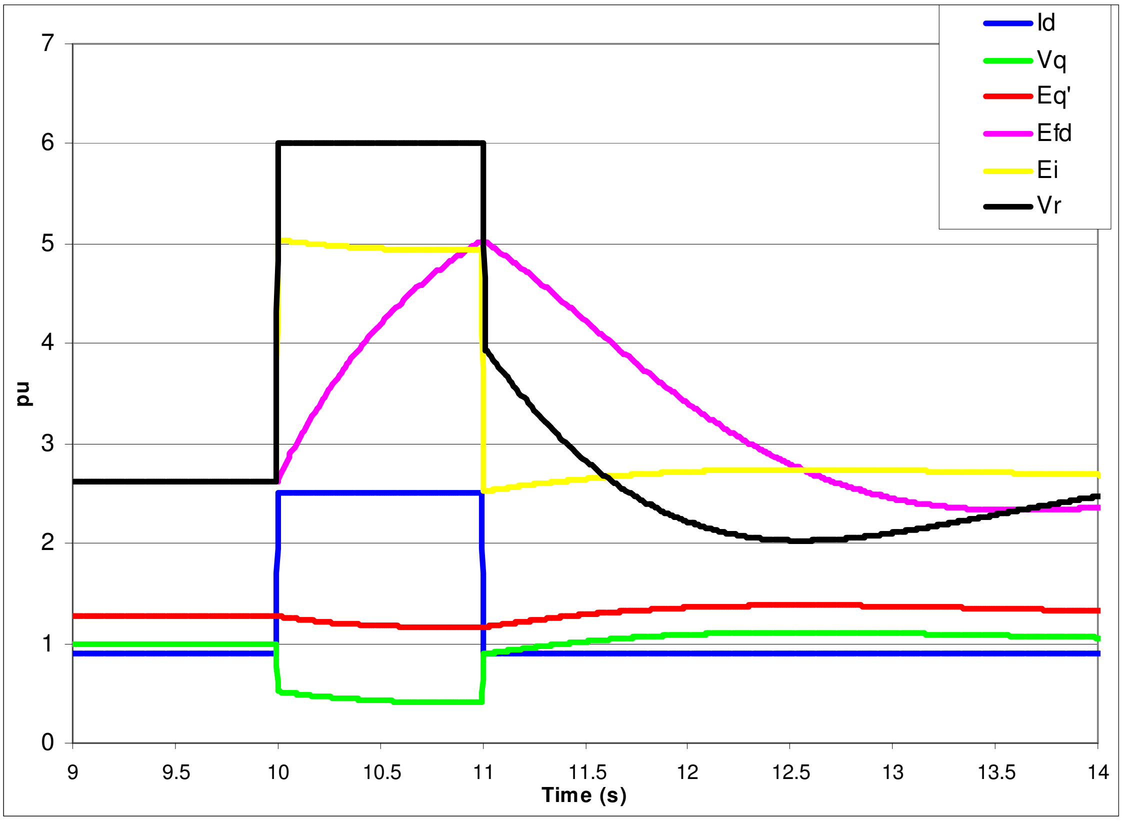

Figure 2.25: Generator EMF E_q' plotted against E_{fd} and E_{xc}

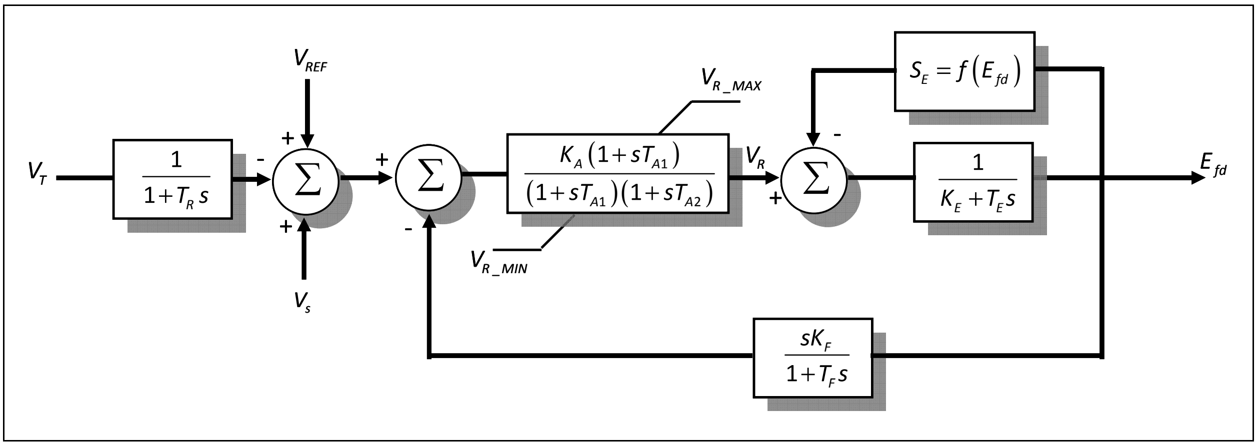

Figure 2.26: Rotating brushless exciter: IEEE Type DC 1 – adapted from [6] and [47]

Figure 2.26 shows a typical block diagram of an excitation system with a brushless rotating main exciter, where the constants have the following meaning:

T_E	Main exciter time constant
V_{RMIN}	Minimum value of Regulator Voltage V_R
V_{RMAX}	Maximum value of Regulator Voltage V_R
K_E	Exciter gain
K_A	Regulator Gain
K_F	Regulator stabilizing circuit gain
T_F	Regulator stabilizing circuit gain time constant
T_A	Regulator time constant
S_E	Exciter saturation

In conclusion, the generator EMF can be assumed to remain constant during a fault of up to 300 ms when a brushless exciter is used. The pre-fault generator EMF $E_q^{'}$ will therefore be used in the stability calculations of the new pole-slip protection function.

2.11 SHAFT TORQUE RELATIONSHIPS

This section investigates the possibility to calculate the generator shaft torque for possible use in the pole-slip algorithm. The steady-state torque on a synchronous machine shaft can be calculated by the following equation:

$$T = \frac{P}{\omega_r} \tag{2.64}$$

The rotational speed of the rotor can be calculated by using the measured voltage (or current) frequency of the machine as follows:

$$\omega_r = \frac{2\pi f}{p} \tag{2.65}$$

where f is the measured voltage (or current) frequency

The electrical centre is defined as the point in the network where the voltage is zero when the transfer angle is 180^0 between the generator EMF and the infinite bus [15]. In an out-of-step scenario, the electrical centre can be in the generator/step-up transformer, or in a long transmission line far away from the generator. It will be shown in equation (3.8) that the current that flows at the electrical centre is equal to the current that would flow when a bolted short circuit is applied at the electrical centre location. When the electrical centre is close to a generator, the effect will be equivalent to that of a bolted short circuit close to the generator during an out-of-step scenario. Therefore, when the electrical centre is close to the generator, the torque on the generator shaft in an out-of-step condition will be higher than when the electrical centre is far away from the generator.

When the rotor torque exceeds the mechanical design limits, the generator must be tripped. Subsynchronous resonance must also be taken into account for cases where the slip does not take place in the generator/step-up transformer, but rather in a long transmission line far away from the generator. In such cases it can be calculated how severe the torque pulsations are on the generator rotor. By knowing whether the machine is operating close to the shaft mechanical strength, an informed decision should be made whether the generator must be tripped, or whether the generator can be kept on-line to improve chances that the whole network can become stable again.

The equations that describe the electrical torque and flux linkage in a synchronous machine are [14]:

$$T_e = \psi_d i_q - \psi_q i_d \tag{2.66}$$

$$\psi_d = L_d i_d + L_{md}\left(i_{fd} + i_{kd}\right) \tag{2.67}$$

$$\psi_q = L_q i_q + L_{mq}\left(i_{kq1} + i_{kq2}\right) \tag{2.68}$$

It can be seen from equation (2.67) that the direct-axis flux linkage (ψ_d) is dependant on the excitation current (i_{fd}) and the damper winding current (i_{kd}). The damper winding current will only be present during transient conditions. The *transient* torque on the shaft will be higher than the torque calculated by equation (2.65) due to the effect of the damper windings. With a higher excitation current, the pull-out torque on the shaft will also increase.

Figure 2.27 shows the torque curves of a 600 MW generator during a bolted three-phase fault on the step-up transformer HV terminals. The fault is applied at t = 10 s and cleared at t = 10.2 s. The torque, as simulated by PSCAD, differs considerably from the calculated torque in equation (2.64), since the transient damper winding effects are not included in equation (2.64).

Figure 2.28 shows the torque curves of a 600 MW generator during a single phase-to-phase fault on the step-up transformer HV terminals. It can be seen that the torque curve has a second harmonic component during the single-phase-to-phase fault. The single-phase-to-phase fault torque is also higher than the three-phase fault torque. The single-phase-to-phase fault is a more severe fault due to the higher frequency of torque pulses on the shaft. A single-phase-to-phase fault transient torque is even higher than the instant when the fault is cleared as can be seen in Figure 2.28. The new pole-slip protection function will not be able to protect the generator from the transient torque effect (one cycle) at the instant that the fault occurs, but it can trip the generator before the fault clears to avoid the post-fault pulsating torques on the shaft.

It can be seen from Figure 2.27 and Figure 2.28 that equation (2.64) is not sufficiently accurate to calculate transient torque magnitudes. Due to the complexity of modelling the transient torque behaviour of a generator, it is more practical to trip the generator only when it is predicted that the generator will become unstable after a fault. The machine must be tripped before the fault is cleared to avoid the post-fault pulsating torques as shown in Figure 2.27 and Figure 2.28.

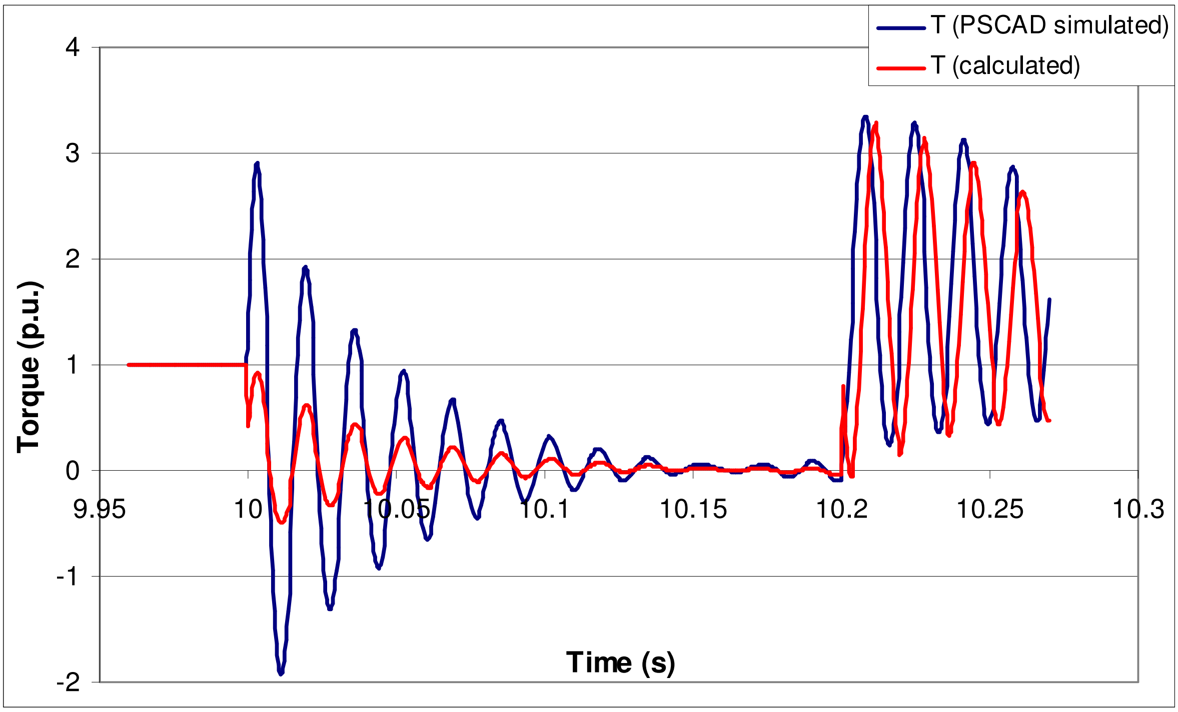

Figure 2.27: Torque curves of a generator due to a 3-phase fault on the step-up transformer HV terminals

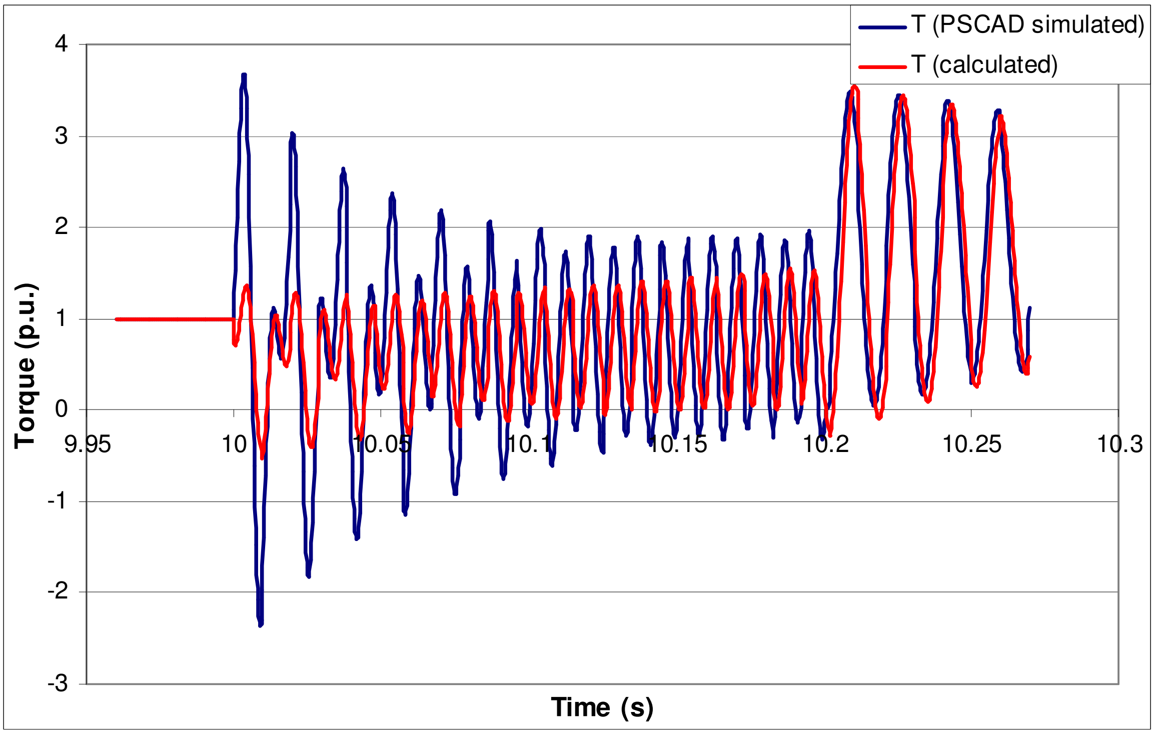

Figure 2.28: Torque curves of a generator due to a phase-to-phase fault at the step-up transformer HV terminals

2.12 TORQUE MAGNITUDE FOR ELECTRICAL CENTRE LOCATION DURING POWER SWINGS

The term “rest of the network” is used when the rest of the network can be modelled as a large generator that is connected at the other end of the transmission line to which the generator under consideration is connected.

The location of the electrical centre is determined by the impedance of the transmission lines, the generator, and the step-up transformer as well as the voltage magnitudes of the generation units. When the transmission line impedance is large compared to the generator and transformer impedances, the electrical centre will typically fall within the transmission line. Section 3.4 describes how the electrical centre location is not only dependant on network impedances, but on the voltage magnitudes in the network as well.

Figure 2.29 shows the torque curves for a 600 MW synchronous generator during a phase-to-phase fault on the step-up transformer secondary side with *short* transmission lines between the generator and the rest of the network. With the short transmission lines, the electrical centre falls within the generator/step-up transformer during out-of-step conditions. It can be seen from Figure 2.29 that the torque on the generator shaft after the fault is cleared is approximately 3.5 pu.

Figure 2.30 shows the torque curves of the same generator under the same fault conditions as in Figure 2.29, but with longer transmission lines between the generator terminals and the rest of the network. The peak torque at the instant when the fault occurs is similar for the short and long transmission line scenarios. The important difference in torque is when the fault is cleared. When the fault is cleared, the shaft torque is considerably higher with the short transmission lines than with the long transmission lines scenario.

The electrical centre for Figure 2.29 is located close to the generator (due to the short transmission line), while the electrical centre for Figure 2.30 is located further away from the generator during the power swing.

As discussed in section 2.11, the aim is to predict machine stability to trip the machine before the fault is cleared. This will avoid the post-fault stress on the rotor, especially when the electrical centre is located close to the generator during the power swing.

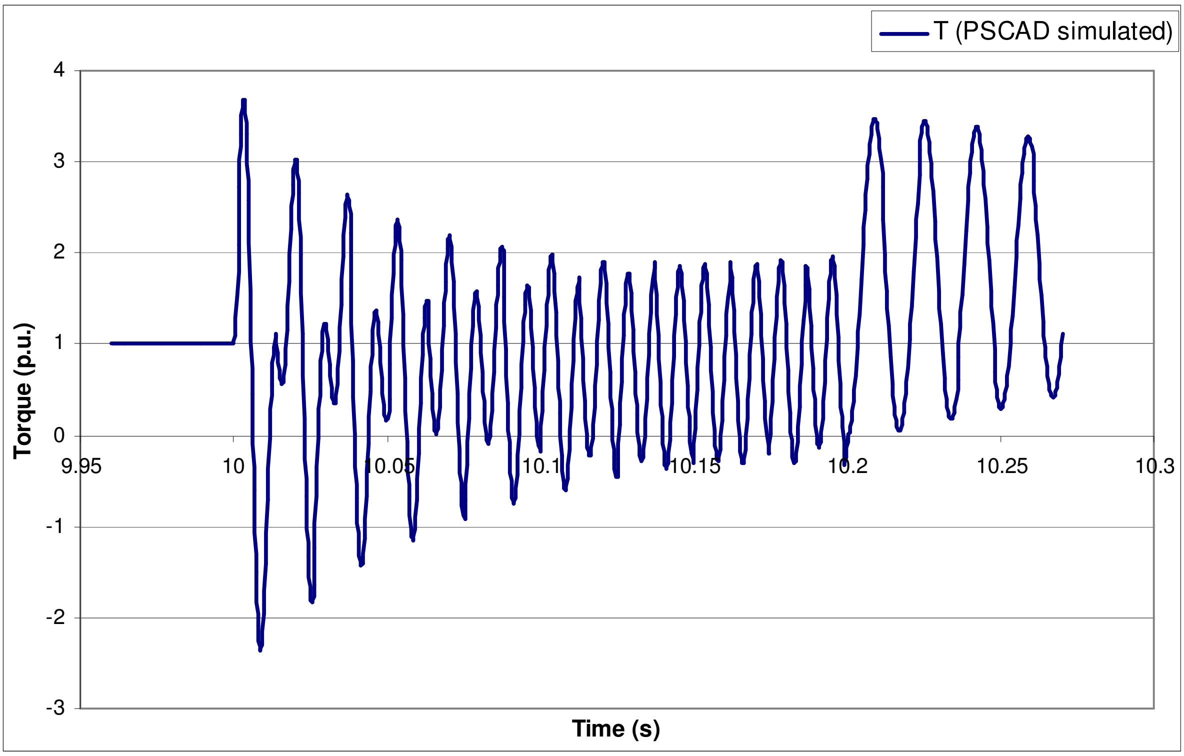

Figure 2.29: Torque curves of a large generator due to a phase-to-phase fault at the step-up transformer HV terminals with a short transmission line

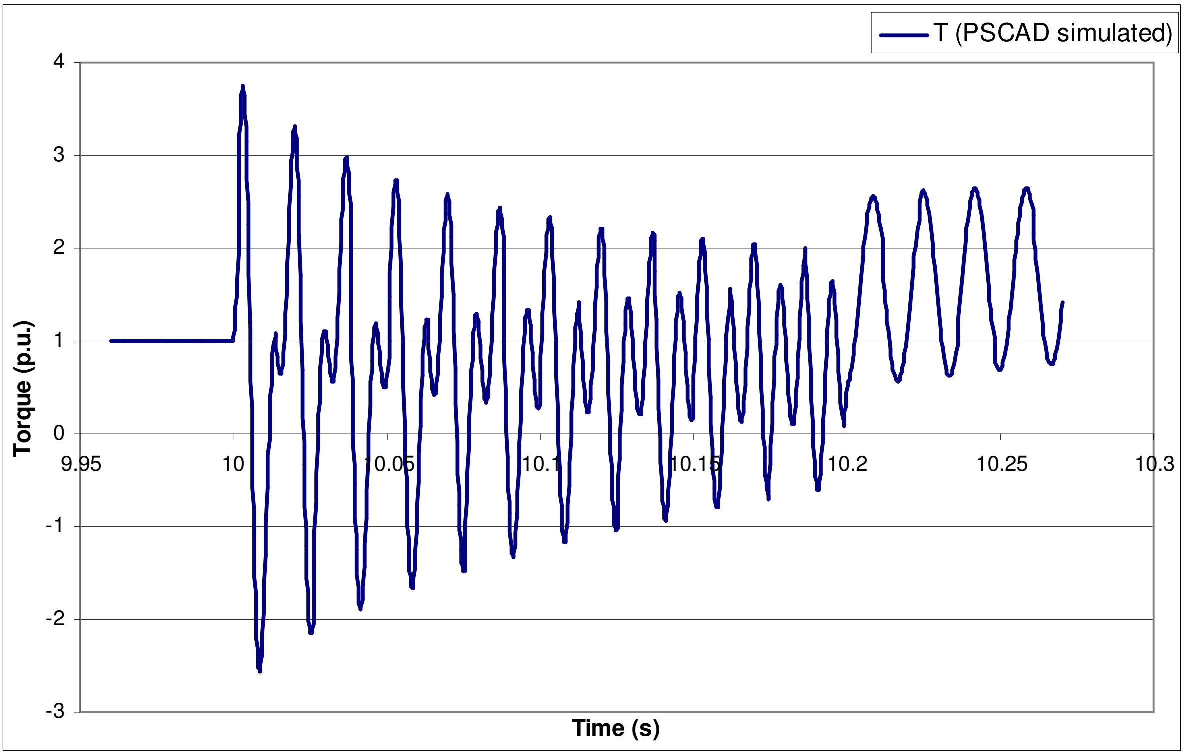

Figure 2.30: Torque curves of a large generator due to a phase-to-phase fault at the step-up transformer HV terminals with a long transmission line

2.13 MECHANICAL SHAFT STRESS CALCULATIONS

The shear stress on the generator shaft must be considered during the shaft design process to ensure that the shaft will be able to deliver rated power. The shaft must also be able to withstand short-circuit faults and pole-slip scenarios. The steady-state torque (T) on the shaft is:

$$T = \frac{P}{\omega_r} \tag{2.69}$$

The shear stress (τ) on the shaft is calculated as follows [18:123]:

$$\tau = \frac{T \cdot d}{2 \cdot J} \tag{2.70}$$

where T is the torque on the shaft [$N.m$]

d is the diameter of the shaft [m]

J is the polar second moment of area [m^4]

Figure 2.31 explains the variables used in equation (2.70). The polar second moment of area (J) is calculated as follows:

$$J = \frac{\pi \cdot d^4}{32} \tag{2.71}$$

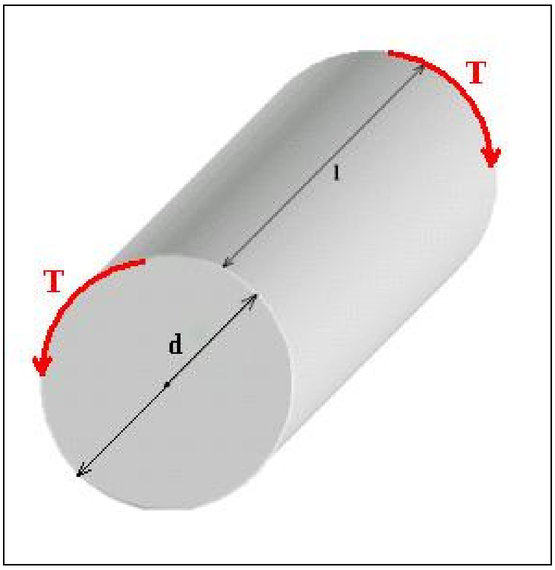

Figure 2.31: Shaft with dimensions and torque indicated

Figure 2.32 shows the fatigue strength (S_f) vs. the number of stress cycles (N) for UNS G41300 steel [18:368]. The maximum continuous torque (not pulsating) that a synchronous machine shaft can withstand is typically 12 pu [46]. From equation (2.70) it can be seen that the shear stress is directly proportional to the torque applied to the shaft. For this reason the value of S_{ut} in Figure 2.32 can be chosen to be 12 pu.

The fatigue strength of the material reduces as the stress cycles are increased. When the applied stress on the shaft is less than the endurance limit (S_e), failure will not occur, no matter how great the number of cycles.

The endurance limit of Carbon steels, Alloy steels and Wrought irons is shown in Figure 2.33. Table 2.2 also provides endurance limits of some Carbon and Alloy steels. It can be seen that the endurance limit ratio (S_e/S_{ut}) is between 0.23 and 0.67.

Table 2.2: Endurance limit ratio Se/Sut for various steel microstructures [18:368]

	Ferrite	***Pearlite***	***Martensite***
Carbon steel	0.57-0.63	0.38-0.41	-
Alloy steel	-	-	0.23-0.47

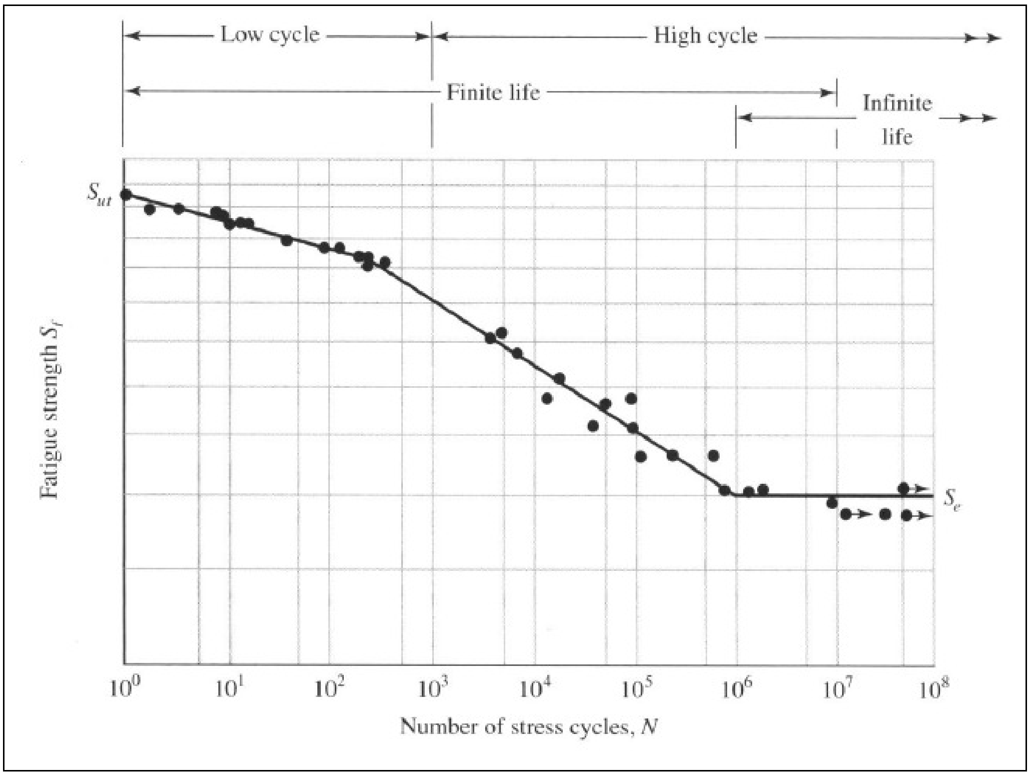

Figure 2.32: Fatigue strength (kpsi) vs. stress cycles for UNS G41300 steel [18:368]

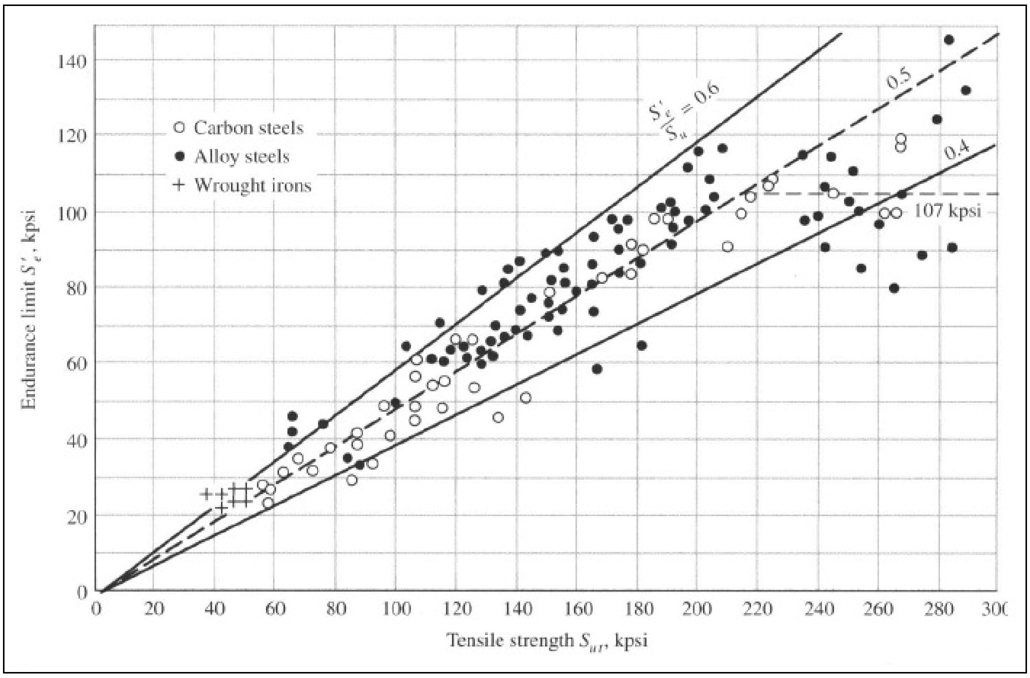

Figure 2.33: Endurance limit vs. tensile strength for various materials [18:369]

The pole-slip protection function must trip the synchronous machine when the shaft stress is higher than the endurance limit S_e. When pole slipping occurs, with the shaft stress below the endurance limit S_e, the machine need not be tripped immediately. If the machine is not tripped, there is a better chance that the network can become stable again.

Since the endurance limit of different machine shafts will vary depending on the design, a *conservative* endurance limit of S_e/S_{ut} = 0.2 (from Table 2.2) could be implemented in the pole-slip protection function. This means that the maximum allowable shaft torque is calculated as follows:

S_{rated} = 1 pu (design or rated stress)

Endurance limit ratio:

$$\frac{S_e}{S_{ut}} = 0.2 \tag{2.72}$$

$$\begin{aligned} \therefore S_e &= 0.2 \times S_{ut} \\ &= 0.2 \times 12 \\ &= 2.4 \quad pu \end{aligned} \tag{2.73}$$

For any stress (or torque) greater than 2.4 pu, the machine should be tripped.

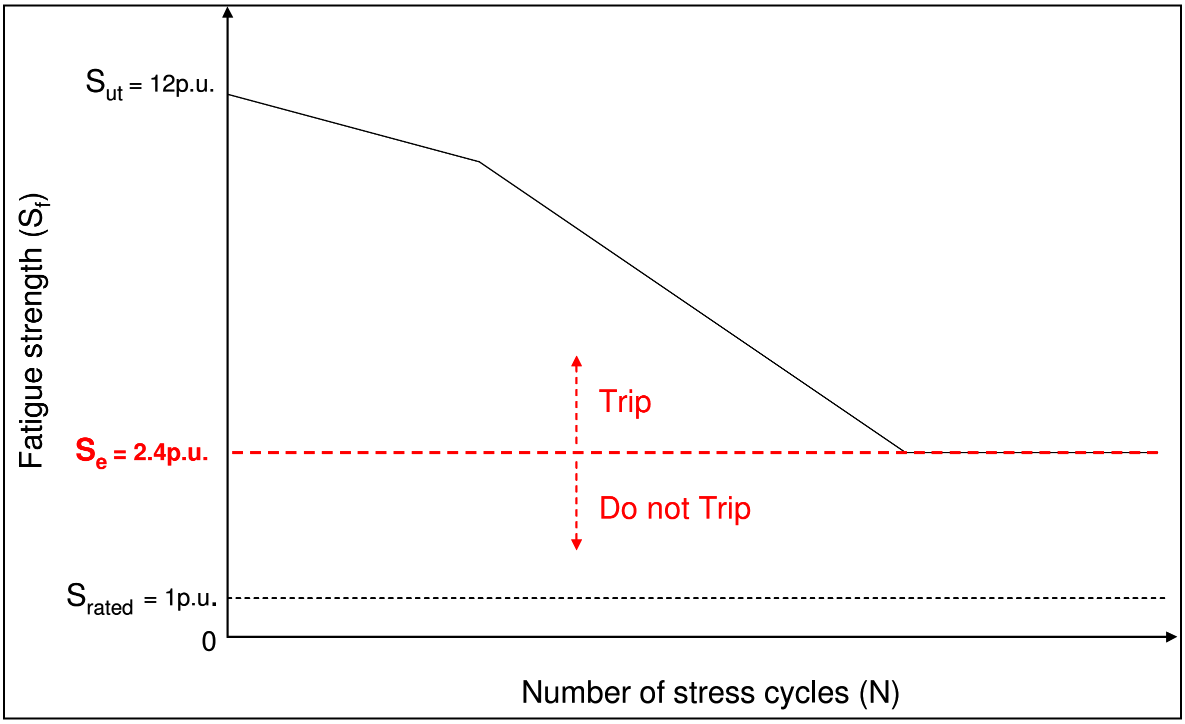

Figure 2.34: Synchronous machine shaft fatigue strength trip limit

It is important to note that it would not be practical to trip the generator for every shaft torque value greater than 2.4 pu. When the generator remains stable after the fault torque is in excess of 2.4 pu, the generator should rather stay on-line to maximize overall network stability. If it can be predicted that the generator will fall out-of-step (become unstable) after the fault is cleared, the generator should be tripped as soon as possible.

It was shown in section 2.11 that the calculation of shaft torque as presented in equation (2.69) cannot accurately determine transient torque during the fault. After the fault is cleared, the torque calculated by equation (2.69) is reasonably accurate and could be used to determine subsynchronous resonance effects on the shaft after a disturbance. Section 2.14 provides more detail on subsynchronous resonance.

2.14 Subsynchronous Resonance

The formal IEEE definition of Subsynchronous resonance (SSR) is [19]:

“Subsynchronous resonance is an electric power system condition where the electric network exchanges energy with a turbine generator at one or more of the natural frequencies of the combined system below the synchronous frequency of the system”

The most common cause of subsynchronous resonance is transmission lines that have series capacitors to compensate for the transmission line inductance. The transmission lines with the series LC combinations have natural frequencies ω_n that are defined as follows [20:4]:

$$\omega_n = \sqrt{\frac{1}{LC}} = \omega_B \sqrt{\frac{X_C}{X_L}} \tag{2.74}$$

where ω_n is the natural frequency associated with a particular line LC product

ω_B is the system base frequency (or rated frequency)

X_L is the transmission line inductive reactance

X_C is the transmission line capacitive reactance

The frequencies appear to the generator rotor as modulations of the base frequency, giving both subsynchronous and supersynchronous rotor frequencies. It is the subsynchronous frequency that may interact with one of the natural torsional modes of the turbine-generator shaft. This can create a condition for an exchange of energy at a subsynchronous frequency, with possible torsional fatigue damage to the turbine-generator shaft [20:4].

The torsional modes (frequencies) of shaft oscillation are usually known, or may be obtained from the turbine-generator manufacturer. The network frequencies depend on many factors, such as the amount of series capacitance in service and the network switching arrangement at a particular time. The presence of subsynchronous torques on the rotor causes concern because the turbine-generator shaft itself has natural modes of oscillation that are typical of any spring-mass system. The shaft oscillatory modes are at subsynchronous frequencies. Should the induced subsynchronous torques coincide with one of the shaft natural modes of oscillation, the shaft will oscillate at this natural frequency, sometimes with high amplitude. This is called subsynchronous resonance, which can cause shaft fatigue and possible damage or failure.

The subsynchronous resonance effects shown in Figure 2.35 have the following meanings [21]:

H is the inertia constant

K is the shaft spring constant

T_m is the mechanical torque on the turbines

T_e is the electrical torque on the generator

γ is the angle of twist between adjacent masses

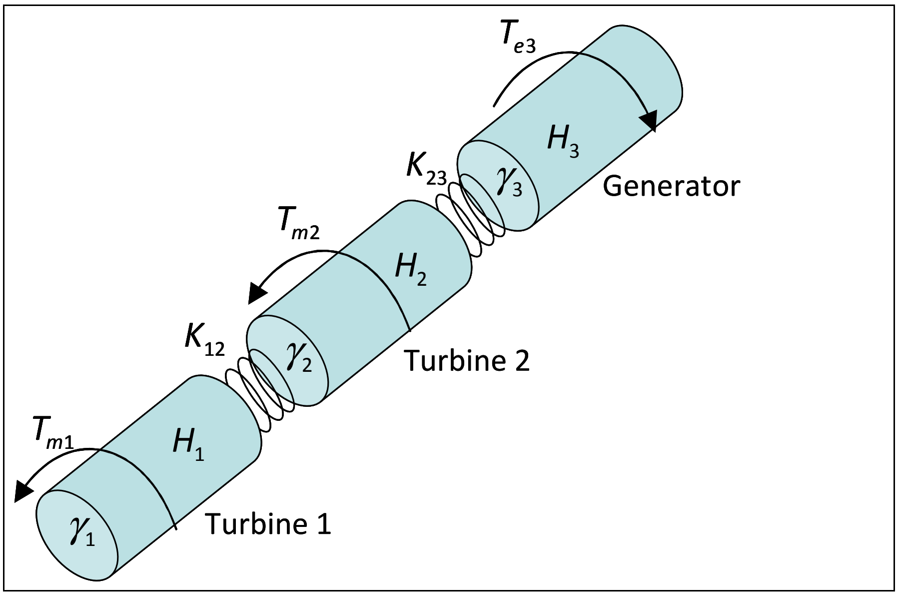

Figure 2.35: Spring-mass system for modelling subsynchronous resonance [21]

Springs represent the ability of the shaft to twist elastically. The torque exerted by the springs is proportional to the relative mechanical angles between adjacent masses. The angle γ can be calculated as follows [18:123]:

$$\gamma = \frac{Tl}{GJ} \tag{2.75}$$

In addition, two damping coefficients are included: The self-damping coefficient creates a torque on the specified mass, which is proportional to its own speed (friction and windage). This torque is applied in steady-state as well as in transient conditions.

The mutual damping coefficient creates a torque, which is proportional to the difference in speed from one mass to the next. The coefficient will not produce torques in steady state, but will damp out oscillations between masses. The torque effects on the generator shaft that are caused by subsynchronous resonance can be calculated by using equation (2.69). *Equation (2.69) can however not determine the resonance torque effects between Turbine 1 and Turbine 2 in Figure 2.35.*

Due to the complexity of determining pulsating torques in the different stages of the turbine system, it was decided not to include the effects of subsynchronous resonance in the pole-slip function. It is recommended in chapter 7 that further fields of study should include the effects of subsynchronous resonance during pole-slip conditions.

2.15 SUMMARY

This chapter discussed the basic theory of synchronous machines. Machine conventions were reviewed to determine the signs of variables like torque, speed and others to be used in the pole-slip protection function. It was concluded that it is important to include the effect of saliency in the generator model for stability calculations. Equations were derived that can be used to determine the steady-state power angle for a synchronous machine.

A basic approach to excitation systems was also given to understand the transient response of the machine EMF during disturbances. It was found that the transient EMF of a synchronous machine does not vary considerably during a fault of short duration (up to 300 ms). It was concluded that the pre-fault transient EMF will be used in the pole-slip protection function.

It was explained in detail why round rotor generators need to be modelled with a transient quadrature axis reactance $X_q^{'}$ and why salient pole generator models do not include $X_q^{'}$. Due to the presence of $X_q^{'}$ in round rotor generator models, a new reactance was introduced, namely X_{q_avg}. The intent of this new reactance is to use it in the equal area criteria that forms part of the new pole-slip protection function.

Shaft torque stress during pole-slip scenarios was investigated to determine the mechanical stress effect of pole slipping on machine shafts. It was concluded that it is not practical to determine transient shaft torque during the fault due to the complexity of the generator model. It was decided that machine stability would rather be predicted to trip the machine before the fault is cleared to avoid the post-fault shaft stresses.

Subsynchronous resonance was briefly introduced. Subsynchronous torques on the shaft between the turbine and the generator shaft can be determined by observing the machine active power fluctuations. Subsynchronous resonance cannot be determined between the different stages of the prime mover by observing electrical parameters like the generator active power. Due to the complexity of determining pulsating torques in the different stages of the turbine system, it was decided not to include the effects of subsynchronous resonance in the pole-slip function.